SARS-CoV-2 nucleocapsid uniquely disrupts chromatin over pathophysiologically relevant gene promoters

Jane M Benoit[1#] and Jonathan H Dennis[1]

1 Department of Biological Science, Florida State University, Tallahassee, FL, USA

Running Head: CoV nucleocapsid induced alteration of host chromatin

#address correspondence to Jane M Benoit, jbenoit@bio.fsu.edu

Graphical abstract

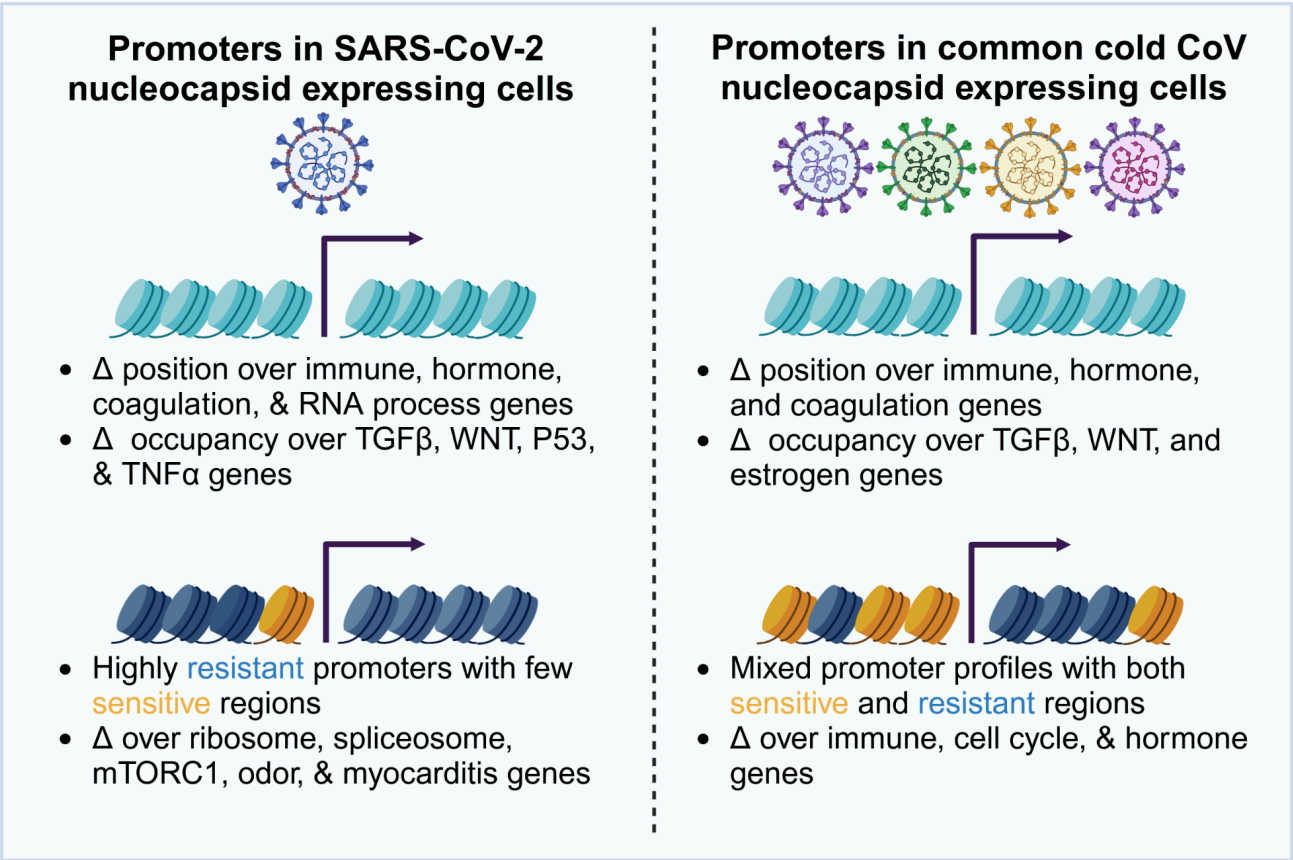

Abstract

SARS-CoV-2, the causative agent of COVID-19, is a positive-sense, single-stranded RNA virus that causes a spectrum of disease severity, from asymptomatic infection to severe illness to long-term sequelae. Similar to other human coronaviruses, SARS-CoV-2 proteins modulate host genomic responses through epigenomic modifications, facilitating viral replication and immune evasion. While the nucleocapsid protein is well known for its role in RNA stability and immune modulation, its impact on host chromatin organization remains unclear. To investigate this, we generated stable human alveolar cell lines expressing nucleocapsid proteins from endemic and pandemic human coronaviruses. Our analysis revealed that nucleocapsid proteins from all tested coronaviruses induced changes in nucleosome positioning and occupancy at specific gene promoters involved in coagulation pathways, hormone signaling, and innate immune responses. Additionally, SARS-CoV-2-specific alterations were identified in genes dysregulated in severe infections, suggesting a direct role for epigenomic modifications in disease pathophysiology. We also observed extensive changes in nucleosome susceptibility to nuclease digestion in SARS-CoV and SARS-CoV-2 samples that were not observed in common cold cell lines. Promoters with altered sensitivity and resistance to nuclease were linked to innate immune, metabolic, olfactory, and signaling pathways known to be dysregulated in severe COVID-19 and post-acute sequelae (PASC). These findings demonstrate that nucleocapsid protein expression alters chromatin structure at specific loci, implicating viral proteins in host genome dysregulation. Furthermore, we identified both shared and unique chromatin targets of SARS-CoV-2 and common cold coronaviruses, highlighting pathways for further investigation and potential therapeutic intervention.

Importance

Host chromatin is known to be modulated by coronaviruses during infections. However, the role of the nucleocapsid protein in these alterations are unknown. Here, we show that nucleocapsids from seven human coronaviruses alter nucleosome distribution and susceptibility to enzymatic digestion over specific gene promoters in a human lung cell line. Nucleocapsids from SARS-CoV and SARS-CoV-2 have the most prominent effects which are seen over genes involved in immune responses, metabolism, hormone signaling, and other pathways that are known to be dysregulated in severe COVID-19 and post-acute sequelae of COVID-19.

Introduction

Coronaviruses are single-stranded positive-sense RNA viruses that infect a wide range of organisms including birds and mammals. Members of both the alphacoronavirus and betacoronavirus genera are able to infect humans and have been responsible for three human pandemics in the past two decades (1). There are four known human coronaviruses which are associated with common colds: HCoV-HKU1, HCoV-NL63, HCoV-OC43, and HCoV-229E (2–5). These viruses generally produce mild upper respiratory infections in healthy individuals, are collectively associated with approximately 30% of common colds (6, 7), and have a high seroprevalence in adults (8, 9). Both MERS-CoV and SARS-CoV can cause severe lower respiratory tract disease, leading to acute lung injury, respiratory failure, and death (10–16). In contrast, SARS-CoV-2, the causative agent of COVID-19 (17), produces a range of disease phenotypes from asymptomatic infections to severe disease with some individuals experiencing persistent symptoms in the months and years following infection (18, 19). Severe disease from SARS-COV-2 infection is mediated by dysregulation of immune responses (19–22) and the majority of the global population has been exposed to this virus. HCoV-NL63 and HCoV-229E are both alpha coronaviruses while HCoV-OC43, HCoV-HKU1, SARS-CoV, MERS-CoV, and SARS-CoV-2 are beta coronaviruses (23, 24). Each human coronavirus evolved in animal hosts and independently emerged as a human pathogen (25–27). A large reservoir of coronaviruses in animal populations presents a continued risk of zoonotic spillover into humans (10, 28–30).

Human coronavirus genomes are composed of a linear positive-sense single strand of RNA with two partially overlapping open reading frames encoding structural, accessory, and nonstructural proteins (31–33). The assembled viral particle contains an RNA genome which is coated with nucleocapsid protein and encased in an lipid bilayer embedded with spike, envelope, and membrane proteins (34, 35). Individual CoV proteins have specific functions in the cell which

range from dampening host immune responses to promoting viral replication. CoV infection is known to directly interfere with host cells through disruption of host chromatin organization which leads to dysregulation of gene expression and can have long term consequences for the host cell and organism as a whole (36). Because chromatin architecture tightly regulates gene expression, viral disruption of these structures can profoundly impact cellular function

In eukaryotic cells, linear DNA is packaged within the nucleus as chromatin by wrapping DNA around a core octamer of eight histone proteins to form a nucleosome. Nucleosomes are joined together by linker DNA and are further compacted into chromatin fibers. This compaction compacts the DNA within the nucleus and regulates accessibility to repair, replication, and transcriptional machinery (37–40). Nucleosomes within promoters are especially critical for transcriptional regulation as they act as barriers transcription by preventing assembly of the pre-initiation complex (41) and depletion of nucleosomes results in aberrant expression of otherwise silent genes (42). Highly expressed genes are defined by highly phased nucleosomes flanking a nucleosome depleted region over the immediate transcription start site (TSS) (43–45). Epigenomic modifications of the underlying DNA and chromatin proteins contribute to this regulation without altering the underlying DNA sequence. These modifications include DNA methylation (46–48), histone modifications such as acetylation, methylation, phosphorylation or ubiquitination (49–51), and RNA modifications (52–54). Each of these modifications interact with the overall chromatin architecture and contribute to regulation of gene expression.

Coronaviruses have evolved mechanisms to perturb host chromatin to promote viral replication and limit immune responses on both local and genome wide scales. SARS-CoV and MERS-CoV infection result in altered or delayed interferon gene responses which are regulated through alterations in histone post translational modifications over specific immune response genes (36, 55). HCoV-229E infection also results in altered histone modifications and pol II

recruitment which are associated with differential gene expression (56). Alterations in histone post translational modifications extend to transposable elements which are uniquely modulated following SARS-CoV-2 infection (11). Recent high-throughput CRISPR screens have identified chromatin remodelers, cohesin, and transcription factors as key regulators of host responses to infection, underscoring the role of chromatin organization in viral pathogenesis (57–59). Chromatin accessibility, as measured by ATACseq, is disrupted over immune genes in peripheral blood mononuclear cells from recovering COVID-19 patients (60) and those with severe and mild disease (61, 62) indicating chromatin alterations occur in a variety of disease contexts. SARS-CoV-2 infection alters higher-order chromatin structure, leading to restructuring of HiC A/B compartments. This is accompanied by reduced loop extrusion and increased local variability over immune response genes. These changes are coupled with alterations in HPTM deposition and gene expression (63, 64). Interestingly, these higher order modifications were not observed in infection with HCoV-OC43 (64) but similar patterns of compartment mixing and loss of stability over pro-inflammatory genes are observed in HCoV-229E infection (65) suggesting variability across CoVs. Specific large scale chromatin rearrangements in olfactory cells have been associated with anosmia following SARS-CoV-2 infection in hamsters and humans (66) suggesting functional implications for these chromatin alterations. Individual SARS-CoV-2 proteins have known impacts on host chromatin structure and function. The ORF8 protein functions as a histone mimic (67) and disrupts host gene regulation disrupting histone post translational modifications. NSP1 is a multifunctional protein which disrupts host mRNA translation and stability (68–70), blocks nuclear export (71, 72), antagonizes type I interferon signaling (73), and reduces Pol II occupancy and silences immune genes (74, 75). Other viral proteins have known functions on RNA rather than chromatin such as SARS-CoV-2 nucleocapsid which interacts with genes involved in RNA synthesis, splicing, and stability (76). While prior studies have examined the impact of CoV infections on host chromatin, the direct

effects of the majority of individual viral proteins on nucleosome architecture remain underexplored.

Despite the global importance of coronaviruses and the ongoing risk of future spillovers, their direct effects on chromatin architecture at the nucleosomal scale—one of the most fundamental levels of gene regulation—remain poorly understood. To answer this question, we generated a reductionist system to study the impacts of seven human CoV nucleocapsid proteins on nucleosome architecture in a human lung cell line. We opted to study the nucleocapsid protein as it is highly abundant, generally conserved, and has known roles in RNA regulation but is understudied in the context of chromatin (77). Nucleocapsid contributes to viral RNA replication and stability (78–81) and has broad RNA binding capabilities (82–84). The SARS-CoV-2 nucleocapsid protein induces expression of *Il-6* and other inflammatory cytokines through *NF-Kb* signaling (85, 86), inhibits prevents RIG-I recognition of viral dsRNA (87, 88), and prevents IRF3 phosphorylation to limit type I interferon responses (89). Our reductionist system allowed us to probe the effects of nucleocapsid on chromatin structure which might be overshadowed in an infection model due to wide ranging effects on host cells.

To determine the role of CoV nucleocapsid proteins on nucleosome distribution and susceptibility to enzymatic digestion within promoters, we generated stable A549 human lung epithelial cell lines expressing the full length nucleocapsid proteins of seven human CoVs. Replicate cell lines were generated for each of the following nucleocapsids: HCoV-HKU1, HCoV-NL63, HCoVOC43, HCoV-229E, SARS-CoV, MERS-CoV, and SARS-CoV-2 which were compared to cells expressing an empty vector construct. The distribution of nucleosomes across promoters was determined by digesting crosslinked chromatin with Micrococcal nuclease (MNase), an enzyme which selectively cleaves linker DNA leaving nucleosomal DNA intact for high throughput sequencing (43, 90). In addition to mapping the location of individual

nucleosomes, a titration of MNase was used to determine the susceptibility of a given nucleosome to enzymatic digestion (91–96). This method identifies nucleosomes which are sensitive or resistant to enzymatic digestion and is correlated with gene expression and transcription factor binding suggesting that it is a useful method for identification of active and silent genes. We chose to focus our analysis on promoter regions as nucleosomes within promoter regions have distinct roles in gene regulation, are highly occupied, and are especially well positioned compared to the rest of the genome.

Our results indicate that SARS-CoV-2 nucleocapsid expression specifically alters nucleosome positioning and occupancy at genes involved in immune response, coagulation, and hormone signaling—pathways linked to severe COVID-19 outcomes and post-acute sequelae. Many of these genes are differentially expressed in severe acute disease and continue to be dysregulated in post acute sequelae (PASC) months following infection. In contrast, we identified greater disruptions in susceptibility to nuclease digestion with unique alterations occurring in both common cold and pandemic viruses. SARS-CoV-2 specific alterations were localized over genes associated with tight junction interactions, innate immune signaling, and endocrine pathways. Our findings reveal distinct alterations in nucleosome distribution and nuclease sensitivity upon expression of SARS-CoV-2 nucleocapsid in a controlled reductionist system. Affected genes were associated with disease phenotypes and may offer insight into the pathophysiology of both common cold and pandemic CoVs.

Results

Nucleosome distribution over promoters is largely stable in cells expressing CoV nucleocapsids

To investigate the impact of coronavirus (CoV) nucleocapsid proteins on nucleosome architecture, we generated A549 human lung alveolar cell lines expressing nucleocapsid genes from seven human CoVs: 229E, NL63, HKU1, OC43, MERS-CoV, SARS-CoV, and SARS-CoV-2. While these nucleocapsid proteins share conserved functions, they exhibit distinct amino acid sequences (Supp. Fig. 1) and can be classified into alphacoronaviruses, common cold betacoronaviruses, and pandemic betacoronaviruses (Fig. 1A). To ensure the correct integration of full-length wild-type nucleocapsid genes, we validated all cell lines through Sanger sequencing.

To assess nucleosome positioning, we digested crosslinked chromatin with Micrococcal nuclease (MNase) and isolated mononucleosome-sized DNA fragments for nucleosome mapping (workflow shown in Fig. 1B). A combination of light and heavy MNase digests allowed us to capture nucleosomes with varying susceptibility to nuclease cleavage (Fig. 1C). Using a previously validated promoter sequence capture approach (97, 98) , we enriched for nucleosomes within 2 kb of RefSeq transcription start sites (TSSs), achieving strong enrichment over Pol II promoters with robust coverage from libraries containing as few as 20 million reads per sample (Supp. Fig. 2).

Comparative analysis revealed that nucleosome distribution across Pol II promoters was highly similar between CoV nucleocapsid-expressing and empty vector control cell lines. The Spearman's correlation coefficient exceeded 0.89 for nucleosome distribution signals across 100-bp bins, indicating high overall similarity between samples (Fig. 1D). Furthermore,

aggregate nucleosome maps across all samples (Fig. 1E) demonstrated a conserved promoter architecture, including: 1. Four weakly phased but highly occupied upstream nucleosomes 2. A prominent nucleosome-depleted region (NDR) over the TSS 3. A strongly positioned and highly occupied +1 nucleosome 4. Four weakly phased but highly occupied nucleosomes downstream of the TSS. Although variability was observed in the phasing and occupancy of individual nucleosomes, the overall promoter nucleosome architecture remained consistent across conditions. These patterns align with previously reported human nucleosome distribution maps (43, 93, 94, 97, 98), supporting the robustness of our findings.

Nucleosome positioning and occupancy is altered over specific gene promoters in cells expressing CoV nucleocapsids

Although overall nucleosome distribution remained highly similar across samples, statistical analysis revealed CoV-specific alterations in nucleosome positioning and occupancy when compared to empty vector controls. Nucleosome positioning refers to the location of a nucleosome relative to the underlying DNA, whereas occupancy is defined by the summit value of the nucleosome peak. To identify changes in positioning, we used DANPOS3 (102) to compare nucleosome positions in CoV nucleocapsid-expressing cell lines with those in empty vector controls. High-confidence repositioning events were defined as a shift of >80 bp in summit position which was consistent across replicates. Across conditions, we identified between 119 to 361 genes with at least one repositioned nucleosome in their promoter regions (Fig. 2A, Table 2). Notably, the majority of repositioned genes were unique to each CoV nucleocapsid, with limited overlap between common cold CoVs and pandemic CoVs (Fig. 2A, Supp. Table 1).

Among genes with nucleosome repositioning unique to SARS-CoV, we identified PABPC1, a gene involved in RNA transport, translation, and stability. The Polyadenylate-binding protein 1 (PABPC1) has been previously reported to interact with the SARS-CoV-2 nucleocapsid (76, 109). Gene ontology (GO) analysis of promoters with repositioned nucleosomes across CoV nucleocapsid conditions revealed associations with innate immune signaling, coagulation, hormone responses, and signaling pathways (Supp. Fig. 3). Additionally, many of these genes overlap with known dysregulated genes in SARS-CoV-2 infection and severe disease progression, further supporting a potential functional relationship between CoV nucleocapsid expression, chromatin remodeling, and pathophysiological outcomes.

We next analyzed nucleosome occupancy changes, defining significant alterations as a ≥5-fold increase or decrease compared to empty vector controls, with an FDR and p-value <0.05. High-confidence altered occupancy events were filtered for consistency across replicates. This analysis identified between 412 to 2,548 genes with increased nucleosome occupancy (Fig. 2B, Table 2) and between 134 to 1,717 genes with decreased nucleosome occupancy compared to controls (Fig. 2C, Table 2). Similar to repositioning, most nucleosome occupancy changes were unique to a single nucleocapsid condition, with moderate overlap between common cold and pandemic CoVs (Fig. 2, Supp. Table 2). GO analysis of promoters with increased nucleosome occupancy revealed enrichment in pathways related to TGF-β signaling, WNT signaling, Hedgehog signaling, and estrogen responses (Supp. Fig. 4). These pathways align with previous studies linking these pathways to lung fibrosis, sex differences in disease severity, and other disease pathologies (110–113). Promoters with increased occupancy in SARS-CoV-2-expressing cells also included PABPC1 and LARP1, both of which have established interactions with SARS-CoV-2 nucleocapsid protein, as well as 36 additional genes known to interact with other SARS-CoV-2 proteins (76, 109).

For genes with decreased nucleosome occupancy, GO analysis identified many of the same pathways as those with increased occupancy, along with p53 signaling and TNF-α pathways (Supp. Fig. 5, Supp. Table 3). TNF-α signaling is a major driver of cytokine storm and severe COVID-19 outcomes, reinforcing a potential link between CoV nucleocapsid expression, chromatin remodeling, and immune dysregulation (21, 113–117). Collectively, these results suggest that CoV nucleocapsid proteins induce targeted nucleosome distribution changes at specific gene promoters, many of which are functionally relevant to host response pathways, disease progression, and severe COVID-19 outcomes.

Nucleosome susceptibility to nuclease digestion is associated with active promoters

While nucleosome positioning and occupancy provide key insights into chromatin alterations following CoV nucleocapsid expression, these analyses alone do not fully capture the breadth of pathways affected by CoV infection. Because nucleosome distribution mapping offers a largely static view of chromatin organization, we expanded our analysis to include nucleosome susceptibility to nuclease digestion to better understand gene regulation in infected cells. Using a titration of Micrococcal Nuclease (MNase), we generated light and heavy digests to identify nucleosomes with differential susceptibility to nuclease activity (Fig. 1C). Nucleosomes preferentially released under light digest conditions were classified as “sensitive,” whereas those requiring heavy digestion were labeled “resistant” (summarized in Fig. 3A). This approach has been widely used to characterize promoter chromatin landscapes and distinguish between active and silent genes across various organisms and conditions (91–96).

To establish a baseline chromatin landscape, we analyzed empty vector control cells and assessed the relationship between nucleosome susceptibility and key epigenomic features of

active chromatin. Using publicly available ENCODE datasets (107, 108), we compared nucleosome sensitivity patterns with DNase I hypersensitivity, histone post-translational modifications (PTMs), RNA polymerase II (Pol II) occupancy, and ATAC-seq accessibility (Fig. 3B). This analysis identified several distinct classes of promoters based on their nucleosome sensitivity patterns. Promoters in cluster 1 exhibited diffuse sensitivity, characterized by weakly phased nucleosomes, an occupied nucleosome-depleted region, and reduced levels of H3K27ac, H3K4me3, Pol II, and ATAC-seq signals (Fig. 3B). These promoters were poorly expressed (Fig. 3C), consistent with their repressed chromatin state.

In contrast, cluster 2 promoters displayed a strongly positioned sensitive region over the transcription start site (TSS), a well-defined nucleosome-depleted region, and a strongly positioned +1 nucleosome. This class was hypersensitive to DNase I and exhibited significantly higher levels of H3K4me3, H3K27ac, Pol II, and ATAC-seq signal compared to other clusters (Fig. 3B). As expected given the convergence of active chromatin marks, these promoters were highly expressed (Fig. 3C). These findings suggest that nucleosome sensitivity can be broadly categorized into two functional patterns: diffuse sensitivity, associated with low transcriptional activity, and localized sensitivity over the TSS, linked to highly active promoters.

Both mixed (clusters 3 and 4) and resistant (clusters 5-7) promoter groups showed defined nucleosome-depleted regions and moderate levels of active histone PTMs, Pol II, and ATAC-seq signals (Fig. 3B). These clusters exhibited similar expression levels, with slightly higher transcriptional activity observed in positioned resistant promoters compared to mixed clusters (Fig. 3C). Together, these findings demonstrate that nucleosome susceptibility to MNase digestion distinguishes between active and silent chromatin states. This analysis suggests that nucleosome susceptibility to nuclease digestion can distinguish between active and silent chromatin states. These findings provide a framework for interpreting how alterations

in nucleosome sensitivity following CoV nucleocapsid expression may contribute to transcriptional regulation and disease progression.

The majority of promoters in CoV nucleocapsid expressing cells exhibit altered susceptibility to nuclease digestion

To assess the impact of CoV nucleocapsid expression on chromatin accessibility, we examined nucleosome susceptibility to nuclease digestion across all nucleocapsid-expressing cell lines. Unlike nucleosome distribution, which remained relatively consistent, susceptibility to nuclease digestion was highly variable across cell lines. Pairwise Spearman's correlations over promoter regions ranged from 0.24 to 0.57, indicating substantial differences in chromatin accessibility between conditions (Fig. 4A). When mapping susceptibility across all Pol II promoters, we observed widespread disruption of both sensitive and resistant regions (Fig. 4B). In empty vector control cells, promoter susceptibility followed distinct patterns, including diffusely sensitive, highly positioned sensitive, mixed, positioned resistant, and diffusely resistant groups (clusters 1–7). These patterns were largely preserved in common cold CoVs but were severely disrupted in MERS, SARS-CoV, and SARS-CoV-2 nucleocapsid-expressing cells (Fig. 4B).

This disruption did not result from a global loss of susceptibility but rather from nucleosomes transitioning between sensitive, neutral, and resistant states at specific genomic locations. Quantification of the proportion of sensitive and resistant nucleosomes in each sample confirmed that nucleocapsid-expressing cell lines retained similar or even greater levels of sensitivity and resistance compared to the empty vector control (Table 3). Independent clustering of each sample revealed the emergence of new susceptibility patterns in MERS, SARS-CoV, and SARS-CoV-2 conditions (Fig. 4C). While common cold CoV samples largely maintained the prominent promoter classes seen in control cells, MERS-expressing cells displayed an expanded diffusely sensitive promoter group and a reduction in

mixed-susceptibility promoters (Fig. 4C, compare MERS to null). SARS-CoV-expressing cells exhibited a loss of resistant nucleosomes, an increase in mixed promoter classifications, and the disappearance of the highly positioned sensitive cluster over the TSS (Fig. 4C, compare SARS-CoV to null). Similarly, SARS-CoV-2-expressing cells lacked the TSS-sensitive cluster and showed an increased proportion of strongly resistant promoters (Fig. 4C, compare SARS-CoV-2 to null). Together, these findings indicate that CoV nucleocapsid expression alters nucleosome susceptibility in a virus-specific manner, with the most pronounced disruptions occurring in MERS, SARS-CoV, and SARS-CoV-2 conditions.

To further investigate the functional consequences of these chromatin alterations, we tracked the movement of genes between promoter classes across conditions. The majority of genes within the diffusely sensitive and silent promoter class were unique to the MERS-expressing cells, reflecting the expansion of this cluster (Fig. 5A, compare MERS cluster 1, Supp. Table 4). The second-largest gene group was common across all conditions, with gene ontology (GO) analysis revealing enrichment for pathways related to coagulation cascades and interferon-gamma responses (adj. p-value < 0.05, MSigDB Hallmark GO database). Additionally, 282 genes in this promoter class were unique to SARS-CoV-2 and were enriched for GO terms associated with olfactory transduction and viral myocarditis (KEGG GO database). Notably, genes transitioning from active mixed or resistant promoter classes in control cells to silent promoter classes in SARS-CoV-2 samples suggest potential transcriptional downregulation driven by SARS-CoV-2 nucleocapsid expression.

The highly expressed TSS-sensitive promoter class was absent in SARS-CoV and SARS-CoV-2 samples. Genes within this class were largely condition-specific, but a subset was shared across all common cold CoVs (Fig. 5B, Supp. Table 5). GO analysis showed significant enrichment for ribosome- and spliceosome-related functions, as well as coronavirus disease pathways (adj. p-value < 0.005, KEGG GO database). The absence of this cluster in SARS-CoV

and SARS-CoV-2 samples suggests a distinct chromatin regulatory mechanism over these promoters, potentially contributing to gene repression in these conditions.

For subsequent analyses, all resistant promoter classes were combined due to their similar gene expression and epigenomic profiles. The majority of genes within resistant promoter classes were shared across all conditions (Fig. 5C, Supp. Table 6) and were significantly enriched for pathways associated with apical junctions, KRAS signaling, and myogenesis (MSigDB Hallmark GO database). However, SARS-CoV-2-expressing cells exhibited an expansion of resistant promoter classes, leading to an increase in SARS-CoV-2-specific genes within this group. These genes were enriched for GO terms related to Myc targets, protein secretion, oxidative phosphorylation, and mTORC1 signaling (MSigDB Hallmark GO database). Overall, these findings indicate that CoV nucleocapsid expression induces widespread alterations in nucleosome susceptibility to nuclease digestion, with potential consequences for transcriptional regulation and disease phenotypes. The pronounced disruptions observed in MERS, SARS-CoV, and SARS-CoV-2 samples suggest virus-specific mechanisms of chromatin remodeling, which may underlie differential pathogenicity and host responses.

Discussion

Human coronavirus (CoV) infections are known to induce epigenomic alterations in host cells, including modifications to histone post-translational modifications (11, 36, 55, 56), altering accessibility as measured by ATACseq (60–62), and disrupting higher order chromatin architecture (63–66). These alterations influence gene expression and may contribute to both short- and long-term cellular dysfunction, even after viral clearance. Individual viral proteins can affect chromatin biology by acting as histone mimics (67), disrupting signaling pathways leading to transcription factor translocation to the nucleus (73, 88, 89, 118), altering RNA stability (68–70, 76, 78), and altering pol II occupancy (74, 75). Here, we systematically compare the effects of human CoV nucleocapsids on nucleosome distribution and susceptibility to nuclease digestion across all human pol II promoters. We identify substantial alterations in nucleosome occupancy over key loci involved in innate immune signaling and other pathways linked to severe disease. Additionally, widespread changes in susceptibility to nuclease digestion are observed in SARS-CoV and SARS-CoV-2 nucleocapsid-expressing cells, particularly over highly expressed genes. These findings suggest that CoV nucleocapsid expression results in remodeled promoter landscapes, potentially contributing to disease outcomes.

We identified 119 to 361 genes with repositioned nucleosomes in their promoter regions, with most repositioning events occurring in a single nucleocapsid-expressing cell line. Gene ontology analysis linked these promoters to innate immune signaling, coagulation, hormone responses, and insulin signaling pathways across multiple CoV samples, with specific disruptions observed at known disease-associated loci such as PABPC1 (76, 109). Additionally, 412 to 2,548 promoters exhibited increased nucleosome occupancy compared to empty vector controls, with gene ontology analysis highlighting enrichment in TGFβ, WNT, hedgehog, and estrogen

signaling pathways—all of which are implicated in CoV disease pathology (110–113). Conversely, 134 to 1,717 promoters showed decreased nucleosome occupancy, primarily affecting genes associated with P53 signaling and TNFα pathways, both of which have known roles in CoV disease progression

(113–117). These results are especially interesting when we consider that nucleosomes can function as barriers (41) and removal of nucleosomes can lead to aberrant expression of otherwise silenced genes (41, 42). This aligns with previous findings that SARS-CoV-2 nucleocapsid significantly upregulates P53 and TNFα signaling in a reductionist model (119) as we would predict from our nucleosome data.This suggests that nucleosome occupancy changes may precede transcriptional alterations in key disease-relevant pathways.

We also observed that susceptibility to nuclease digestion was moderately impacted by common cold CoV nucleocapsids but was severely disrupted in SARS-CoV and SARS-CoV-2 samples. The most striking alterations were observed in a highly active promoter class characterized by a positioned sensitive region at the transcription start site (TSS), which was absent in SARS-CoV and SARS-CoV-2 samples. Genes in this cluster are associated with ribosomal function and the spliceosome, both of which are directly or indirectly affected by SARS-CoV and SARS-CoV-2 (120–122). In SARS-CoV-2 nucleocapsid-expressing cells, promoters linked to olfactory transduction and viral myocarditis shifted from a silent, diffusely sensitive class to a more active, resistant state, suggesting possible gene de-repression with potential implications for anosmia and myocarditis associated with SARS-CoV-2 infection (66, 123–126). Additionally, promoters transitioning from sensitive or mixed susceptibility patterns to a resistant state in SARS-CoV-2 nucleocapsid-expressing cells were associated with Myc signaling, protein secretion, oxidative phosphorylation, and mTORC1 signaling—all of which are dysregulated in SARS-CoV-2 infections (127–131). These findings indicate that pandemic CoVs

induce widespread alterations in promoter susceptibility to nuclease digestion and suggest that these chromatin changes may contribute to disease phenotypes via gene dysregulation.

Our study is the first to evaluate the effects of SARS-CoV-2 and other human CoV nucleocapsids on nucleosome distribution and nuclease susceptibility across all human pol II promoters. We demonstrate that nucleocapsids impact promoter architecture in a reductionist system, with disease-relevant gene classes being particularly affected. Furthermore, common cold CoVs exhibit similar chromatin effects, while SARS-CoV and SARS-CoV-2 nucleocapsids induce more pronounced disruptions in nuclease susceptibility. Beyond providing deeper insights into the functional impact of CoV nucleocapsid proteins on chromatin remodeling, our findings offer a framework for future studies investigating other viral proteins or nucleocapsids from additional viral variants.

Methods

Plasmid design and molecular cloning

Mammalian expression vectors encoding nucleocapsid genes from SARS-CoV-2, OC43, NL63, HKU1, and 229E, driven by a CMV promoter, were obtained from the Ginkgo Bioworks COVID-19 Plasmid Collection via Addgene (Table 1). Custom plasmids for MERS-CoV and SARS-CoV nucleocapsids were synthesized by Twist Biosciences using the same backbone. An empty vector control was generated by Q5-directed mutagenesis (New England BioLabs, #E0554S) of the NL63 construct to remove the nucleocapsid gene. All plasmids were validated via Sanger sequencing of the entire nucleocapsid gene.

Tissue culture and nuclei isolation

A549 lung epithelial cells (ATCC, CCL-185) were cultured in F-12K media (Gibco) supplemented with 10% fetal bovine serum and 1% penicillin-streptomycin and maintained at 37°C with 5% CO_2. Cells were transfected with nucleocapsid or empty vector plasmids (Table 1) using Turbofect (Thermo Scientific) following the manufacturer's protocol. Stably transfected clones were selected with puromycin (Gibco), screened by PCR, and confirmed by Sanger sequencing.

For chromatin analysis, cells were crosslinked with 1% v/v formaldehyde (Sigma-Aldrich) and incubated for 10 minutes at room temperature while rocking. Excess formaldehyde was quenched with 125mM glycine and cells were washed twice in PBS. Cells were resuspended in nuclei isolation buffer (10 mM HEPES at pH 7.8, 2 mM $MgOAc_2$, 0.3 M sucrose, 1 mM $CaCl_2$ and 1% Triton-X) and pelleted by centrifugation at 1000 × *g* for 10 min at 4 °C. Nuclei were washed twice in nuclei isolation buffer and nuclei purity was confirmed by DAPI staining.

MNase cleavage and preparation of DNA libraries

Each condition was processed in biological replicates. For each reaction, 2.5×10^6 nuclei were resuspended in 500 µL of nuclei isolation buffer and digested with Micrococcal Nuclease (MNase) (Worthington) under light (5U) or heavy (200U) conditions for 10 minutes at 37°C. Digestion was stopped with 50 mM EDTA. Protein-DNA crosslinks were reversed by treating MNase-digested nuclei with 0.2 mg/mL proteinase K and 1% SDS, followed by overnight incubation at 65°C. DNA was purified using a guanidinium-isopropanol and ethanol on a silica column.

Mononucleosomal and sub-mononucleosomal DNA (<200 bp) was isolated from a 2% agarose gel and purified by glycogen precipitation. MNase sequencing libraries were prepared using the Accel-NGS®2S Plus DNA Library Kit (Swift) for Illumina®, with a minimum of 10 ng input DNA per digestion. Libraries were indexed using the Accel-NGS 2S Unique Dual Indexing Kit, normalized with Normalase, and quality-checked via D1000 Tapestation. Library molar concentrations were determined via KAPA qPCR and size-corrected using Tapestation data.

Solution-based sequence capture and Illumina sequencing

We used a previously validated Roche NimbleGen SeqCap EZ Library (97, 98) to capture 2kb regions flanking the transcription start site (TSS) of all human genes. TSS sequences were repeat masked with human COT DNA, and library adapters were blocked using universal oligos. Biotinylated capture oligos were hybridized to input libraries for 48 hours and purified with streptavidin beads. Enriched sequences were amplified via 15-cycle PCR using TruSeq primers. Final libraries were assessed via Tapestation, and molar concentrations were determined using KAPA qPCR. Paired-end 50 bp sequencing was performed on an Illumina NovaSeq 6000 at the FSU College of Medicine.

Nucleosome data processing

Raw reads were demultiplexed with Cassava, and adapter sequences and low-quality reads were removed using Trimmomatic (version 0.39) (99). BSequences were aligned to the T2T human genome using Bowtie2 with the --end-to-end --no-mixed --no-discordant flags (100). Mitochondrial and duplicate reads were filtered using Samtools (version 1.10) and Picardtools (version 2.27.3) (101). Read-depth normalization was performed using Picardtools, based on the number of paired-end reads mapping to a 2 kb window centered on the TSS of RefSeq genes. Normalized light and heavy digests were merged using Picardtools to generate total nucleosome profiles. Nucleosome footprints for merged, light, and heavy digests were calculated using DANPOS (version 3.1.1) (102). The $\log_2$ ratio of light to heavy digests was computed at each time point to determine nucleosome sensitivity using deepTools (version 3.5.1) (103).

Nucleosome distribution changes were extracted from DANPOS output using a custom R script with defined cutoffs for repositioning and occupancy alterations. Repositioned nucleosomes were defined as shifts in summit positions >80 bp between conditions. Changes in nucleosome occupancy were identified as $\log_2$ fold changes >5 with a p-value and FDR <0.05 compared to empty vector controls. Only nucleosomes consistently altered across replicates were considered high-confidence and used for further analysis. Statistically significant sensitive and resistant nucleosomes were extracted using another custom R script. Sensitivity was defined by a $\log_2$ fold change in summit score >1.0, while resistance was defined by a fold change <−1.0, with a p-value and FDR <0.05.

Data Visualization and Functional Analysis

Individual loci visualizations were generated using the PlotGardener package (version 1.4.1) in R (version 4.3.2) and the UCSC Genome Browser (104, 105). Additional processing of bigwig files for upset plots was conducted using R (version 4.3.2), bash, and Python3 with custom scripts. Gene ontology enrichment analyses were performed using Enrichr (106) and visualizations were generated with custom R scripts. Publicly available data multi-omics data for A549 cells was obtained from the Encode portal (107, 108) (https://www.encodeproject.org/) with the following identifiers: ENCFF872SDF, ENCFF985FHV, ENCFF541BTE, ENCFF627QMV, ENCFF369ZNM, ENCFF216KUI, ENCFF556OVF, ENCFF425LVX, ENCFF074PND, and ENCFF774RVE.

Data availability

All raw and processed nucleosome occupancy and susceptibility to nuclease files were uploaded to the UCSC genome browser and the NCBI GEO database under accession number GSE290042 (https://www.ncbi.nlm.nih.gov/geo/query/acc.cgi?acc=GSE290042). Basic code for computational analysis from file trimming to nucleosome calling has been provided as a supplemental file (Supp. file 1).

Acknowledgements

We thank Lorea Arambarri, Shahin Behrouz Sharif, and Mahdi Khadem for constructive conversations regarding experimental design and data analysis. This work was supported by the FSU Collaborative Collision COVID-19 Seed Fund. The funders had no role in study design, data collection, data interpretation, or decision to publish this work.

Tables

Table 1. Plasmid constructs used to generate stable cell lines

Addgene #	Plasmid name	insert	Antibiotic resistance
151912	pGBW-m4134902	229E nucleocapsid	puromycin
151960	pGBW-m4134906	OC43 nucleocapsid	puromycin
151957	pGBW-m4134908	NL63 nucleocapsid	puromycin
151948	pGBW-m4134897	HKU1 nucleocapsid	puromycin
151951	pGBW-m4134903	SARS2-CoV-2 nucleocapsid	puromycin
NA	pTwist_SARS1	SARS-CoV-1 nucleocapsid	puromycin
NA	pTwist_MERS	MERS-CoV nucleocapsid	puromycin
NA	pTwist_null	Empty vector	puromycin

Table 2.

Number of genes with one or more re-distributed nucleosomes within 2kb promoter regions in each CoV nucleocapsid cell line compared to empty vector (null).

Time	repositioning	increased occupancy	decreased occupancy
229E	238	910	486
NL63	118	667	133
HKU1	294	1712	1103
OC43	360	2039	296
MERS	188	1109	1716
SARS1	157	411	314
SARS2	284	2547	207

Table 3.

Number and percent of sensitive and resistant nucleosomes within promoters in each CoV nucleocapsid cell line. Nucleosomes with a log2 fold change in summit score greater than 1.5 combined with a p-value and FDR under 0.05 were classified as sensitive if more abundant in light digests and resistant if more abundant in heavy digests. All nucleosomes not meeting these thresholds were classified as neutral.

time	# sensitive	# resistant	# neutral	% sensitive	% resistant
null	25767	19856	131928	14.51	11.18
229E	28386	30888	114402	16.34	17.78
NL63	38165	34514	84282	24.31	21.99
HKU1	49148	47324	68139	29.86	28.75
OC43	29116	28543	110073	17.36	17.02
MERS	16562	15736	125166	10.52	9.99
SARS1	30916	20715	114131	18.65	12.50
SARS2	41455	49218	66946	26.30	31.23

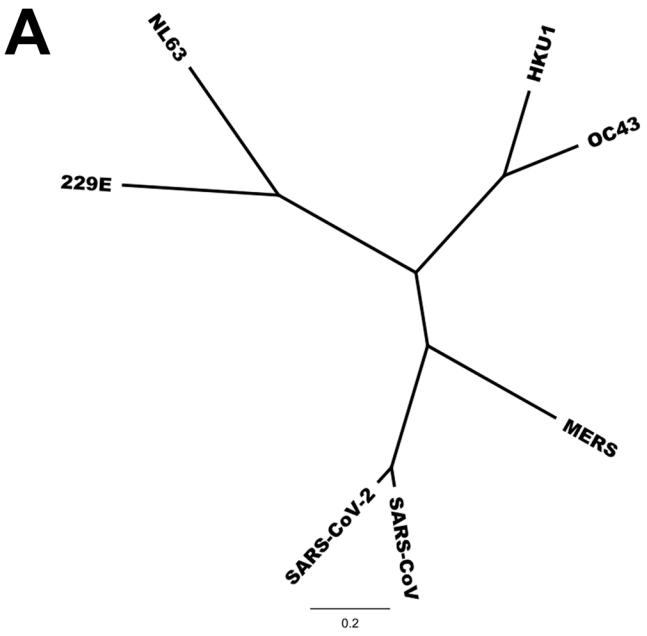
A
NL63
HKU1
OC43
229E
MERS
SARS-CoV-2
SARS-CoV
0.2

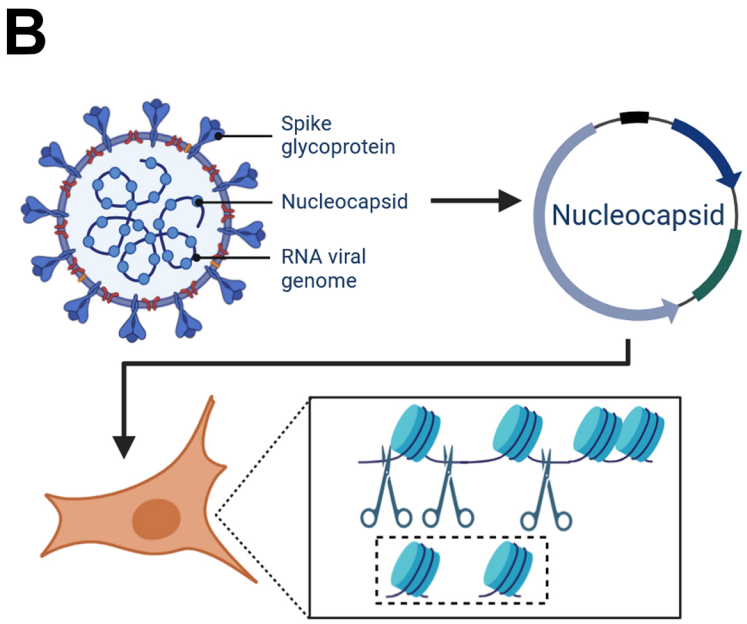
B
Spike glycoprotein
Nucleocapsid
RNA viral genome
Nucleocapsid

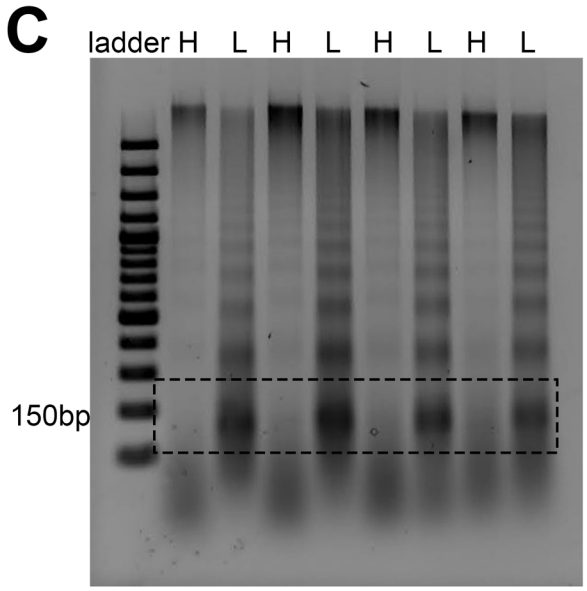
C
ladder H L H L H L H L
150bp

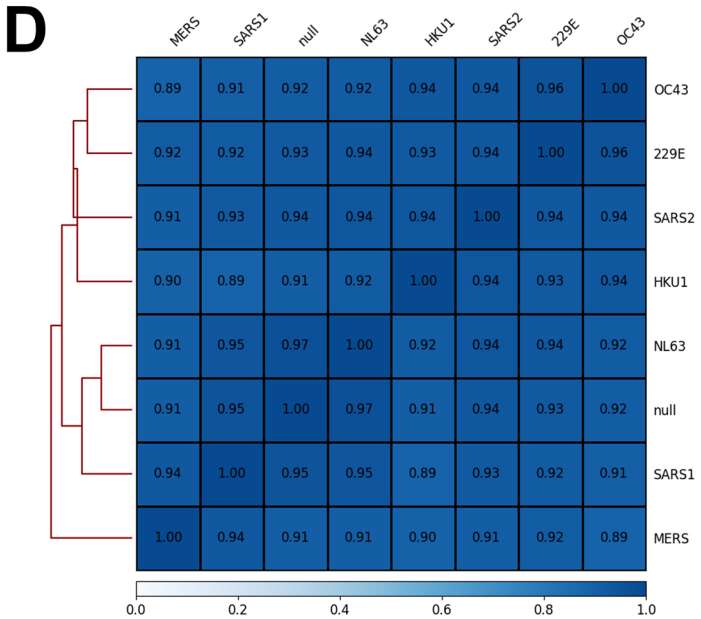
D
MERS SARS1 null NL63 HKU1 SARS2 229E OC43
OC43 0.89 0.91 0.92 0.92 0.94 0.94 0.96 1.00
229E 0.92 0.92 0.93 0.94 0.93 0.94 1.00 0.96
SARS2 0.91 0.93 0.94 0.94 0.94 1.00 0.94 0.94
HKU1 0.90 0.89 0.91 0.92 1.00 0.94 0.93 0.94
NL63 0.91 0.95 0.97 1.00 0.92 0.94 0.94 0.92
null 0.91 0.95 1.00 0.97 0.91 0.94 0.93 0.92
SARS1 0.94 1.00 0.95 0.95 0.89 0.93 0.92 0.91
MERS 1.00 0.94 0.91 0.91 0.90 0.91 0.92 0.89
0.0 0.2 0.4 0.6 0.8 1.0

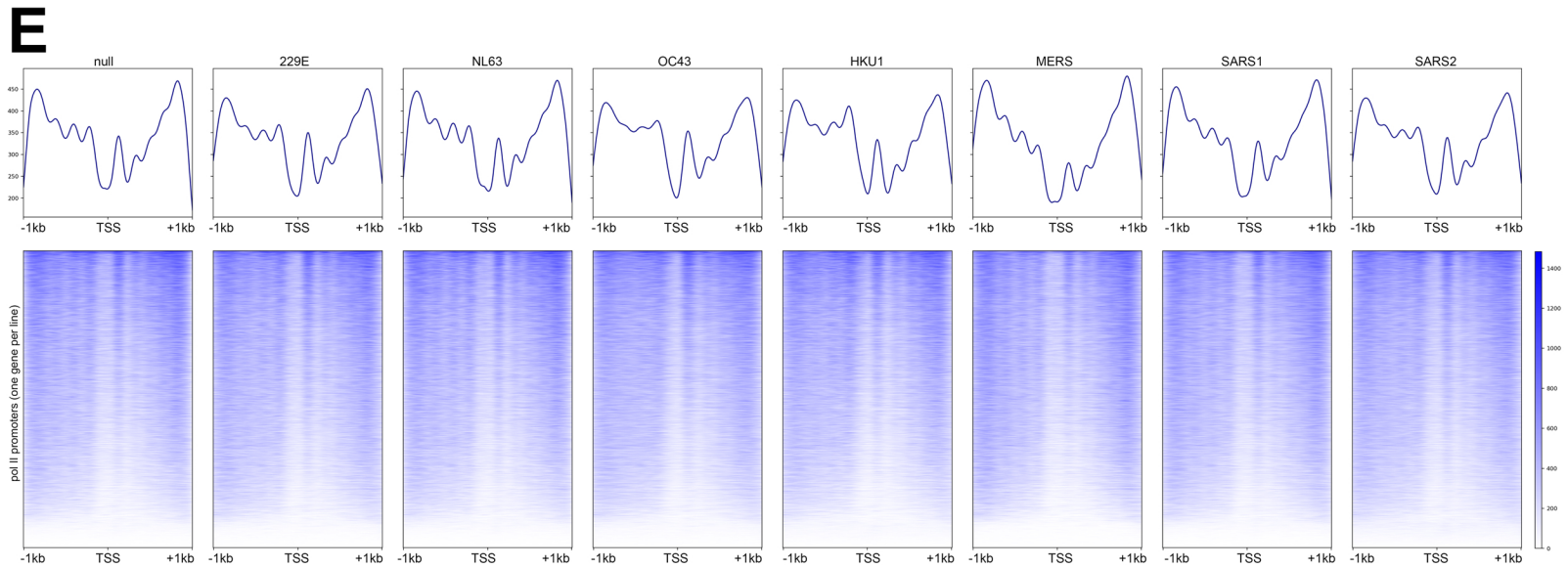
E
null
229E
NL63
OC43
HKU1
MERS
SARS1
SARS2
-1kb TSS +1kb
pol II promoters (one gene per line)

Figure 1. Nucleosome distribution over promoters in CoV nucleocapsid expressing cell lines is highly similar

A. Phylogenetic tree of CoV nucleocapsid proteins generated with a Jukes-Cantor genetic distance model and neighbor joining. Common cold alphaCoVs (229E & NL63), common cold betaCoVs (HKU1 & OC43), and pandemic betaCoVs (MERS, SARS-CoV, & SARS-CoV-2) cluster together. B. Schematic of CoV structure showing nucleocapsid protein. Nucleocapsid genes from six CoVs were engineered into plasmid vectors and expressed in A549 cells. Chromatin from stable cell lines was digested with MNase and mononucleosomal DNA was used to prepare sequencing libraries for mapping experiments. C. Representative agarose gel showing nucleosomal ladders following light (L) ad heavy (H) digests with MNase. D. Spearman correlation between nucleosome signal across 2kb regions of all pol II promoters divided into 100bp bins. Correlation coefficients are listed within each square of the heatmap. E. Heatmaps of nucleosome distribution (blue) over a 2kb region centered on the TSS of pol II promoters (one gene per line) with a line plot showing average signal above each plot. The overall gene order is identical across heatmaps and is determined by maximum signal values.

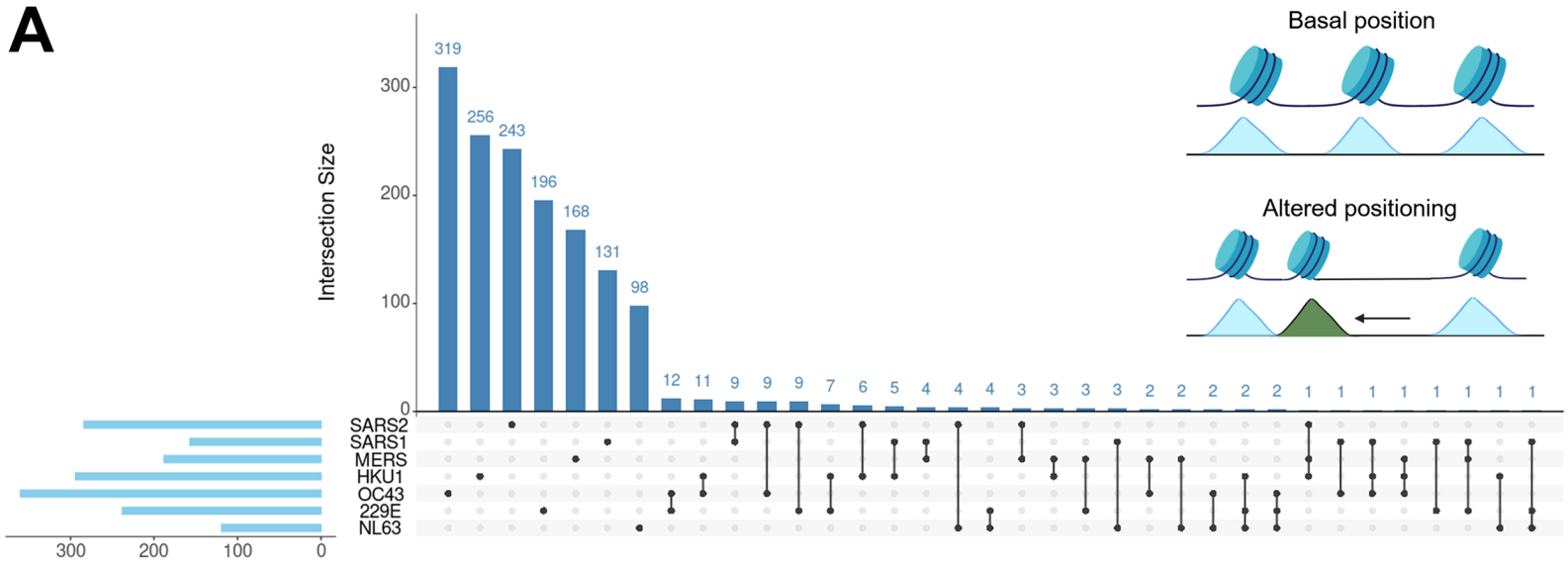
A
Intersection Size
319
256
243
196
168
131
98
12 11 9 9 9 7 6 5 4 4 4 3 3 3 3 2 2 2 2 2 1 1 1 1 1 1 1 1
SARS2
SARS1
MERS
HKU1
OC43
229E
NL63
300 200 100 0
Basal position
Altered positioning

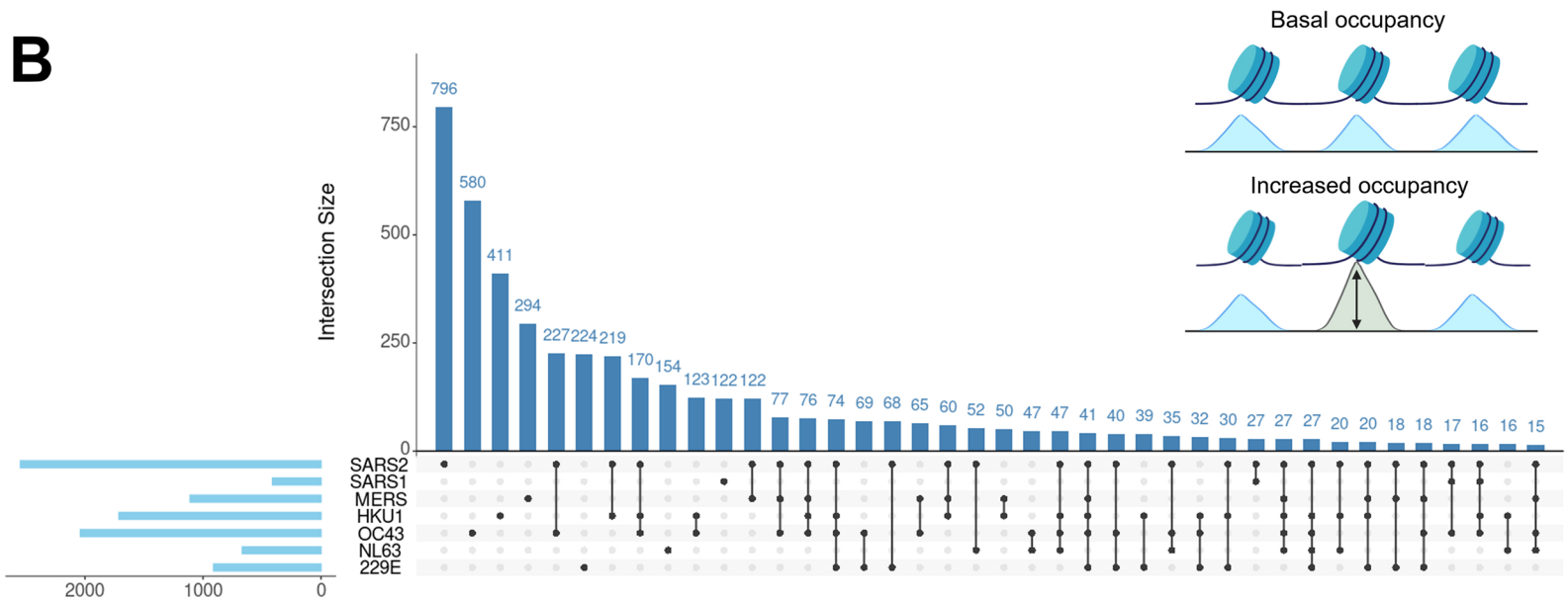
B
Intersection Size
796
580
411
294
227 224 219
170 154
123 122 122
77 76 74 69 68 65 60 52 50 47 47 41 40 39 35 32 30 27 27 27 20 20 18 18 17 16 16 15
SARS2
SARS1
MERS
HKU1
OC43
NL63
229E
2000 1000 0
Basal occupancy
Increased occupancy

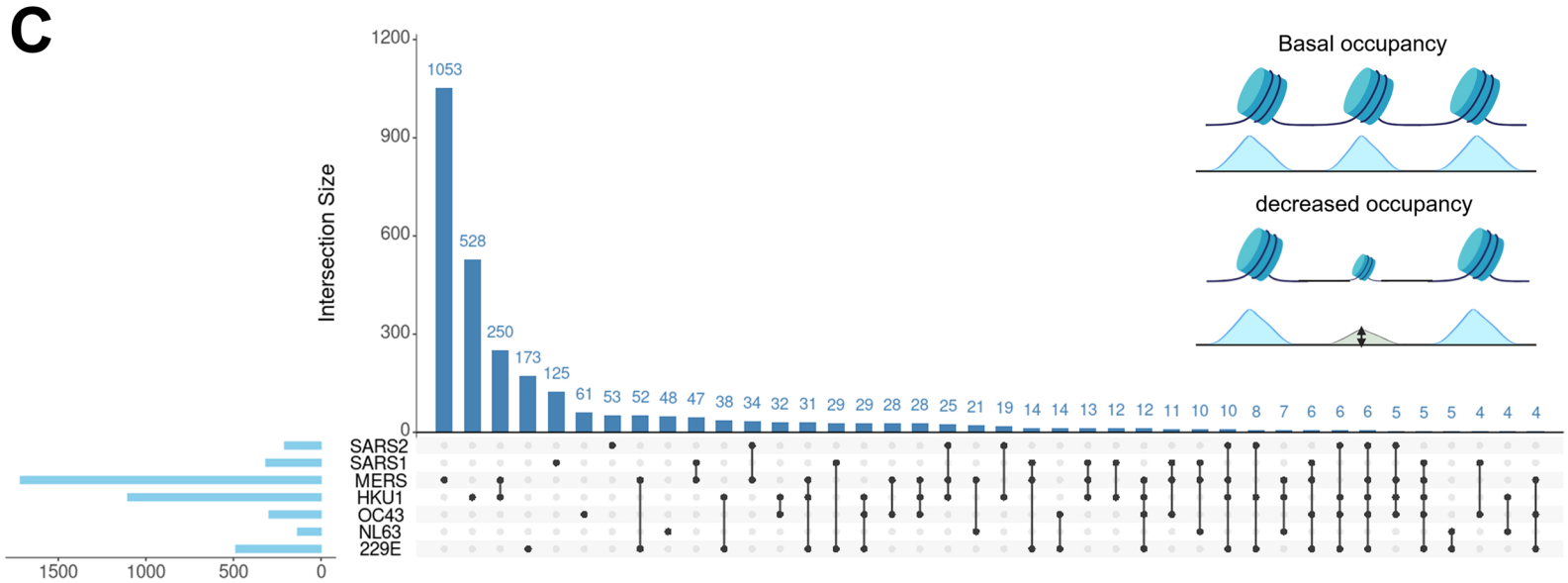
C
Intersection Size
1053
528
250
173
125
61 53 52 48 47 38 34 32 31 29 29 28 28 25 21 19 14 14 13 12 12 11 10 10 8 7 6 6 6 5 5 5 4 4 4
SARS2
SARS1
MERS
HKU1
OC43
NL63
229E
1500 1000 500 0
Basal occupancy
decreased occupancy

Figure 2. Selected promoters in CoV nucleocapsid expressing cells have redistributed nucleosomes

A. Upset plot showing the number of shared and unique genes with one or more nucleosomes with alterations in position (greater than 80bp) across samples. The pale blue horizontal bars show the total number of repositioned nucleosomes while vertical bars and connecting dots show shared genes across samples. B. The same for genes with increased occupancy signal in one or more nucleosomes per gene. C. The same for genes with decreased occupancy signal in one or more nucleosomes per gene.

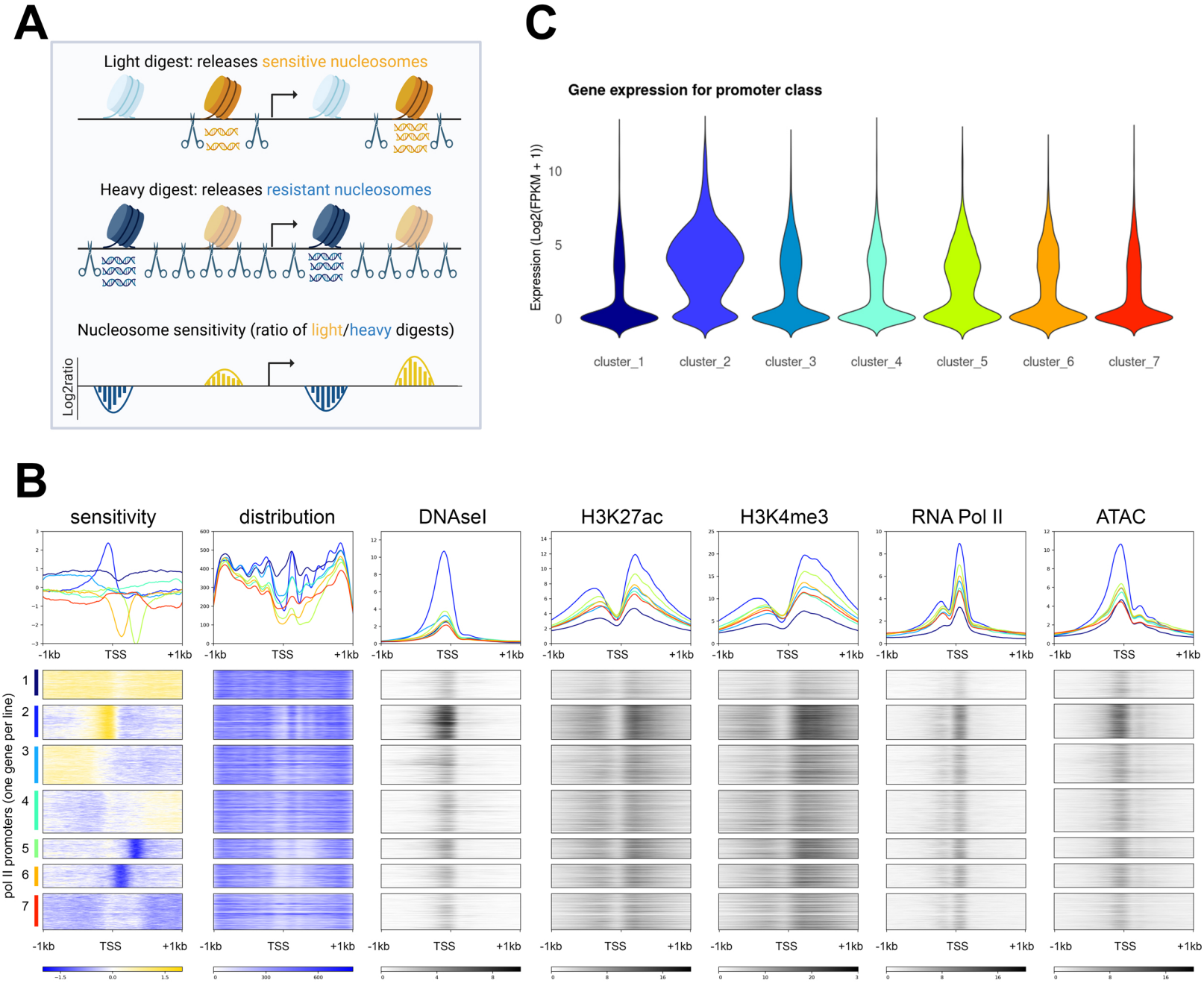
A
Light digest: releases sensitive nucleosomes
Heavy digest: releases resistant nucleosomes
Nucleosome sensitivity (ratio of light/heavy digests)
Log2ratio
C
Gene expression for promoter class
Expression (Log2(FPKM + 1))
cluster_1
cluster_2
cluster_3
cluster_4
cluster_5
cluster_6
cluster_7
B
sensitivity
distribution
DNAseI
H3K27ac
H3K4me3
RNA Pol II
ATAC
-1kb
TSS
+1kb
pol II promoters (one gene per line)

Figure 3. Nucleosome susceptibility to nuclease digestion is associated with active chromatin marks and increased gene expression

A. Schematic of MNase sensitivity assay. A subset of sensitive (gold) nucleosomes are preferentially released under light MNase digest conditions while a different population of resistant (blue) nucleosomes are released under heavy MNase digest conditions. The log2ratio of light over heavy nucleosome signal results in positive values for sensitive nucleosomes and negative values for resistant nucleosomes. B. Heatmap of nucleosome sensitivity (gold) and resistance (blue) over 2kb regions of pol II promoters centered on the TSS for the empty vector sample. Dominant promoter classes were identified by kmeans clustering and gene order is applied to all subsequent heatmaps. Heatmaps of nucleosome distribution signal (blue), DNAseI hypersensitivity signal (black), H3K27ac signal (black), H3K4me3 signal (black), RNA Pol II signal (black), and ATAC signal (black) are sorted by the same gene order as the sensitivity map. Line plots showing the average signal are shown above each heatmap. C. Violin plot of gene expression (log2 (FPKM +1)) for all genes within each sensitivity cluster defined in B.

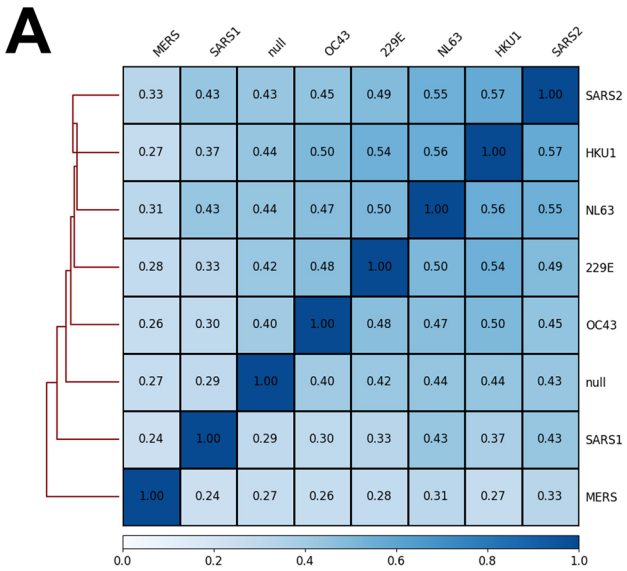
A
MERS SARS1 null OC43 229E NL63 HKU1 SARS2
SARS2 0.33 0.43 0.43 0.45 0.49 0.55 0.57 1.00
HKU1 0.27 0.37 0.44 0.50 0.54 0.56 1.00 0.57
NL63 0.31 0.43 0.44 0.47 0.50 1.00 0.56 0.55
229E 0.28 0.33 0.42 0.48 1.00 0.50 0.54 0.49
OC43 0.26 0.30 0.40 1.00 0.48 0.47 0.50 0.45
null 0.27 0.29 1.00 0.40 0.42 0.44 0.44 0.43
SARS1 0.24 1.00 0.29 0.30 0.33 0.43 0.37 0.43
MERS 1.00 0.24 0.27 0.26 0.28 0.31 0.27 0.33
0.0 0.2 0.4 0.6 0.8 1.0

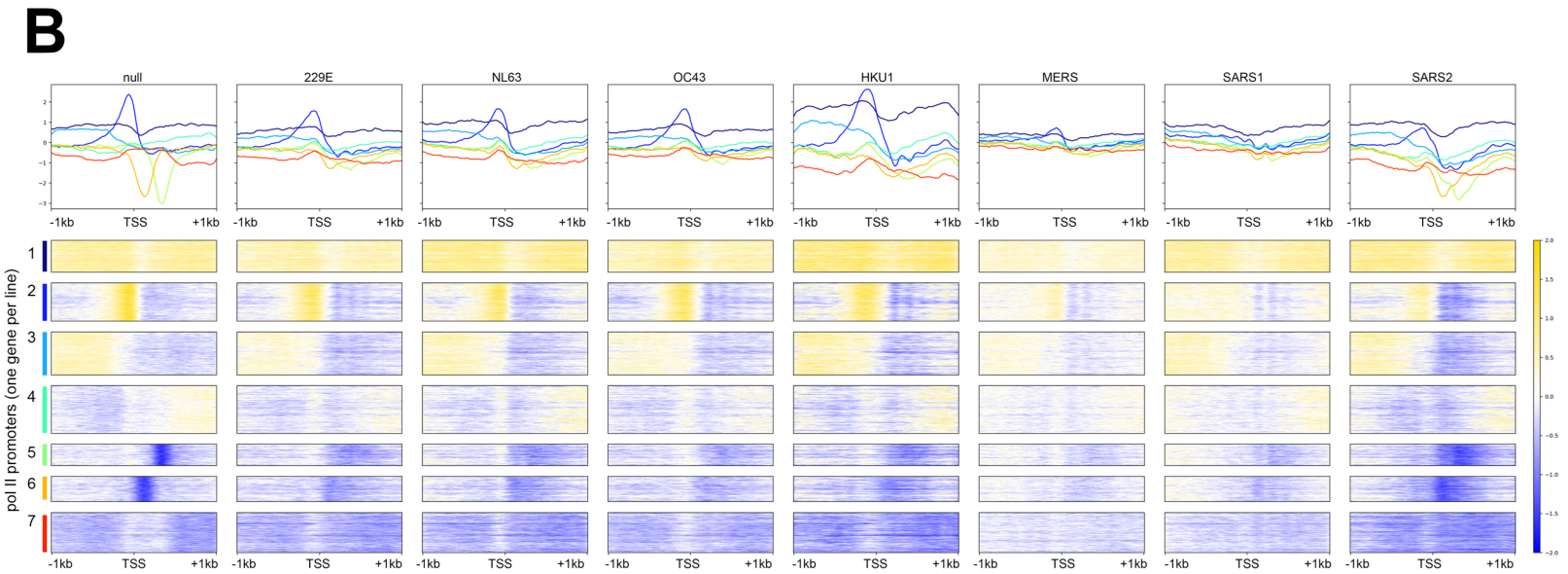
B
null 229E NL63 OC43 HKU1 MERS SARS1 SARS2
-1kb TSS +1kb
pol II promoters (one gene per line)
1 2 3 4 5 6 7

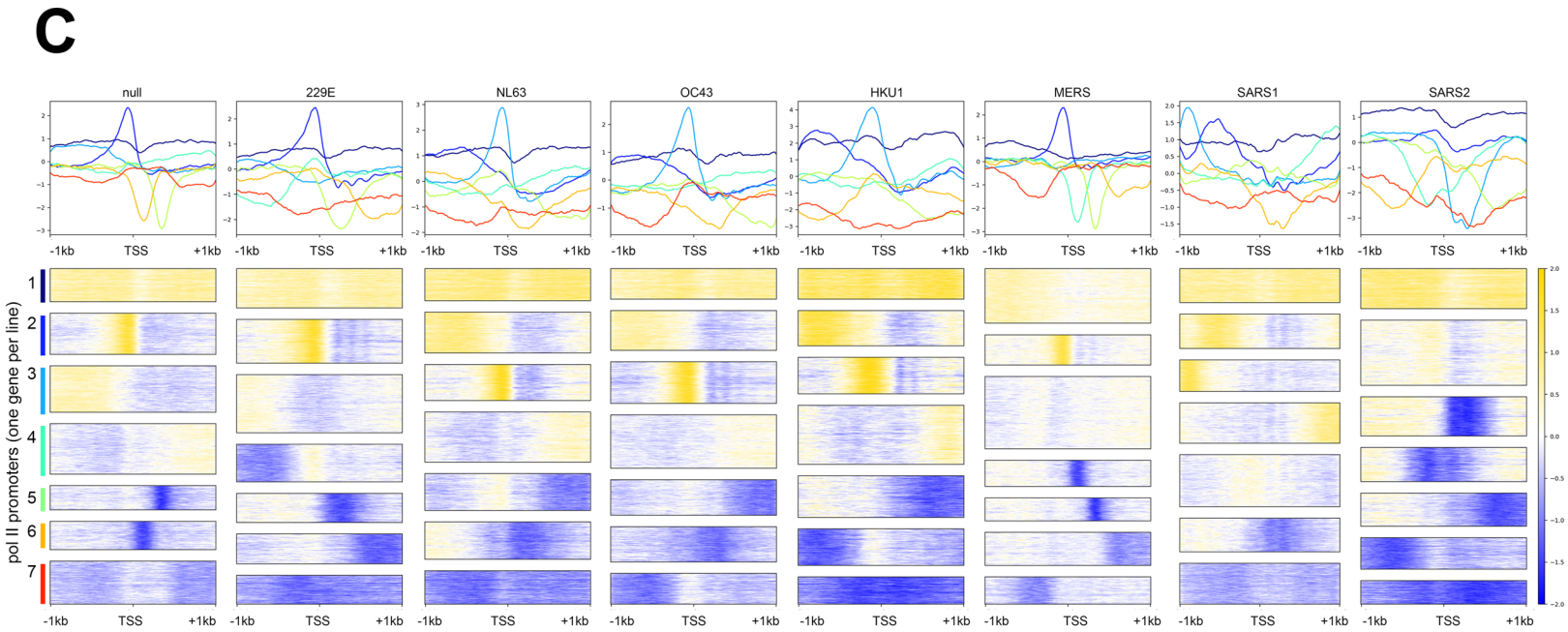
C
null 229E NL63 OC43 HKU1 MERS SARS1 SARS2
-1kb TSS +1kb
pol II promoters (one gene per line)
1 2 3 4 5 6 7

Figure 4. The majority of promoters in CoV nucleocapsid expressing cells have altered susceptibility to nuclease digestion

A. Spearman correlation of nucleosome sensitivity signal over 2kb regions of all pol II promoters divided into 100bp bins. Correlation coefficients are listed within each square of the heatmap. B. Heatmap of nucleosome sensitivity (gold) and resistance (blue) over 2kb regions of pol II promoters centered on the TSS for all samples. Line plots showing the average signal are shown above each heatmap. Kmeans clustering of the empty vector sample was used to establish gene sort order for all samples. C. Heatmap of nucleosome sensitivity (gold) and resistance (blue) over 2kb regions of pol II promoters centered on the TSS for all samples. Kmeans clustering was used to independently generate gene groups for each individual sample. Gene order is accordingly different in each heatmap.

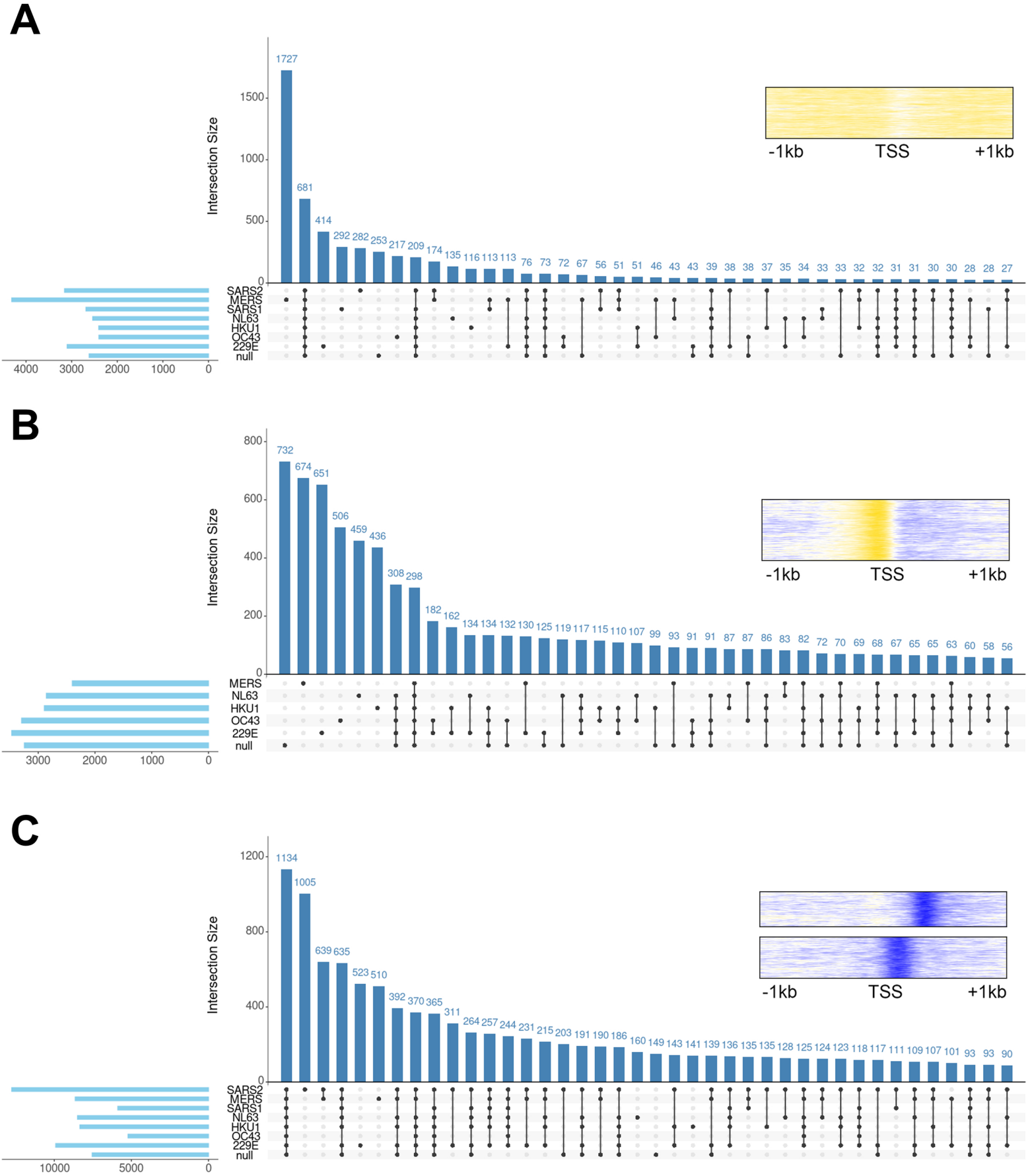
A
Intersection Size
1727 681 414 292 282 253 217 209 174 135 116 113 113 76 73 72 67 56 51 51 46 43 43 39 38 38 37 35 34 33 33 32 32 31 31 30 30 28 28 27
SARS2
MERS
SARS1
NL63
HKU1
OC43
229E
null
4000 3000 2000 1000 0
-1kb TSS +1kb
B
Intersection Size
732 674 651 506 459 436 308 298 182 162 134 134 132 130 125 119 117 115 110 107 99 93 91 91 87 87 86 83 82 72 70 69 68 67 65 65 63 60 58 56
MERS
NL63
HKU1
OC43
229E
null
3000 2000 1000 0
-1kb TSS +1kb
C
Intersection Size
1134 1005 639 635 523 510 392 370 365 311 264 257 244 231 215 203 191 190 186 160 149 143 141 139 136 135 135 128 125 124 123 118 117 111 109 107 101 93 93 90
SARS2
MERS
SARS1
NL63
HKU1
OC43
229E
null
10000 5000 0
-1kb TSS +1kb

Figure 5. Nucleosome susceptibility to MNase is variable across CoV nucleocapsid expressing cell lines

A. Upset plot showing the number of shared and unique genes classified as having diffusely sensitive promoters. The pale blue horizontal bars show the total number of genes in each sample while vertical bars and connecting dots show shared genes across samples. B. Upset plot showing the number of shared and unique genes in the promoter class dominated by a highly positioned sensitive region over the immediate TSS. The pale blue horizontal bars show the total number of genes in each sample while vertical bars and connecting dots show shared genes across samples. C. Upset plot showing the number of shared and unique genes in resistant promoter classes. The pale blue horizontal bars show the total number of genes in each sample while vertical bars and connecting dots show shared genes across samples.

References

1. Hartenian E, Nandakumar D, Lari A, Ly M, Tucker JM, Glaunsinger BA. 2020. The molecular virology of coronaviruses. The Journal of Biological Chemistry 295:12910.

2. Fouchier RA, Hartwig NG, Bestebroer TM, Niemeyer B, de Jong JC, Simon JH, Osterhaus AD. 2004. A previously undescribed coronavirus associated with respiratory disease in humans. Proceedings of the National Academy of Sciences of the United States of America 101.

3. Hamre D, Procknow JJ. 1966. A new virus isolated from the human respiratory tract. Proceedings of the Society for Experimental Biology and Medicine Society for Experimental Biology and Medicine (New York, NY) 121.

4. Woo PC, Lau SK, Chu CM, Chan KH, Tsoi HW, Huang Y, Wong BH, Poon RW, Cai JJ, Luk WK, Poon LL, Wong SS, Guan Y, Peiris JS, Yuen KY. 2005. Characterization and complete genome sequence of a novel coronavirus, coronavirus HKU1, from patients with pneumonia. Journal of virology 79.

5. Da T, Ml B. 1965. CULTIVATION OF A NOVEL TYPE OF COMMON-COLD VIRUS IN ORGAN CULTURES. British medical journal 1.

6. Kim KY, Han SY, Kim HS, Cheong HM, Kim SS, Kim DS. 2017. Human Coronavirus in the 2014 Winter Season as a Cause of Lower Respiratory Tract Infection. Yonsei Med J 58:174–179.

7. Myint SH. 1994. Human coronaviruses: A brief review. Rev Med Virol 4:35–46.

8. Lehmann C, Wolf H, Xu J, Zhao Q, Shao Y, Motz M, Lindner P. 2008. A line immunoassay

utilizing recombinant nucleocapsid proteins for detection of antibodies to human coronaviruses. Diagn Microbiol Infect Dis 61:40–48.

9. Severance EG, Bossis I, Dickerson FB, Stallings CR, Origoni AE, Sullens A, Yolken RH, Viscidi RP. 2008. Development of a nucleocapsid-based human coronavirus immunoassay and estimates of individuals exposed to coronavirus in a U.S. metropolitan population. Clin Vaccine Immunol 15:1805–1810.

10. Graham RL, Donaldson EF, Baric RS. 2013. A decade after SARS: strategies for controlling emerging coronaviruses. Nat Rev Microbiol 11:836–848.

11. Marston JL, Greenig M, Singh M, Bendall ML, Duarte RRR, Feschotte C, Iñiguez LP, Nixon DF. 2021. SARS-CoV-2 infection mediates differential expression of human endogenous retroviruses and long interspersed nuclear elements. JCI Insight 6:e147170.

12. Zhong N. 2004. Management and prevention of SARS in China. Philos Trans R Soc Lond B Biol Sci 359:1115–1116.

13. Peiris JSM, Guan Y, Yuen KY. 2004. Severe acute respiratory syndrome. Nat Med 10:S88–97.

14. de Wit E, van Doremalen N, Falzarano D, Munster VJ. 2016. SARS and MERS: recent insights into emerging coronaviruses. Nat Rev Microbiol 14:523–534.

15. Ksiazek TG, Erdman D, Goldsmith CS, Zaki SR, Peret T, Emery S, Tong S, Urbani C, Comer JA, Lim W, Rollin PE, Dowell SF, Ling A-E, Humphrey CD, Shieh W-J, Guarner J, Paddock CD, Rota P, Fields B, DeRisi J, Yang J-Y, Cox N, Hughes JM, LeDuc JW, Bellini WJ, Anderson LJ, SARS Working Group. 2003. A novel coronavirus associated with severe acute respiratory syndrome. N Engl J Med 348:1953–1966.

16. Zaki AM, van Boheemen S, Bestebroer TM, Osterhaus ADME, Fouchier RAM. 2012. Isolation of a novel coronavirus from a man with pneumonia in Saudi Arabia. N Engl J Med 367:1814–1820.

17. Zhu N, Zhang D, Wang W, Li X, Yang B, Song J, Zhao X, Huang B, Shi W, Lu R, Niu P, Zhan F, Ma X, Wang D, Xu W, Wu G, Gao GF, Tan W. 2020. A Novel Coronavirus from Patients with Pneumonia in China, 2019. The New England journal of medicine 382.

18. Carfì A, Bernabei R, Landi F. 2020. Persistent Symptoms in Patients After Acute COVID-19. JAMA 324.

19. Davis HE, McCorkell L, Vogel JM, Topol EJ. 2023. Long COVID: major findings, mechanisms and recommendations. Nat Rev Microbiol 21:133–146.

20. Schulte-Schrepping J, Reusch N, Paclik D, Baßler K, Schlickeiser S, Zhang B, Krämer B, Krammer T, Brumhard S, Bonaguro L, De Domenico E, Wendisch D, Grasshoff M, Kapellos TS, Beckstette M, Pecht T, Saglam A, Dietrich O, Mei HE, Schulz AR, Conrad C, Kunkel D, Vafadarnejad E, Xu C-J, Horne A, Herbert M, Drews A, Thibeault C, Pfeiffer M, Hippenstiel S, Hocke A, Müller-Redetzky H, Heim K-M, Machleidt F, Uhrig A, Bosquillon de Jarcy L, Jürgens L, Stegemann M, Glösenkamp CR, Volk H-D, Goffinet C, Landthaler M, Wyler E, Georg P, Schneider M, Dang-Heine C, Neuwinger N, Kappert K, Tauber R, Corman V, Raabe J, Kaiser KM, Vinh MT, Rieke G, Meisel C, Ulas T, Becker M, Geffers R, Witzenrath M, Drosten C, Suttorp N, von Kalle C, Kurth F, Händler K, Schultze JL, Aschenbrenner AC, Li Y, Nattermann J, Sawitzki B, Saliba A-E, Sander LE, Deutsche COVID-19 OMICS Initiative (DeCOI). 2020. Severe COVID-19 Is Marked by a Dysregulated Myeloid Cell Compartment. Cell 182:1419–1440.e23.

21. Zhang JJ, Dong X, Cao YY, Yuan YD, Yang YB, Yan YQ, Akdis CA, Gao YD. 2020. Clinical

characteristics of 140 patients infected with SARS-CoV-2 in Wuhan, China. Allergy 75.

22. Silvin A, Chapuis N, Dunsmore G, Goubet A-G, Dubuisson A, Derosa L, Almire C, Hénon C, Kosmider O, Droin N, Rameau P, Catelain C, Alfaro A, Dussiau C, Friedrich C, Sourdeau E, Marin N, Szwebel T-A, Cantin D, Mouthon L, Borderie D, Deloger M, Bredel D, Mouraud S, Drubay D, Andrieu M, Lhonneur A-S, Saada V, Stoclin A, Willekens C, Pommeret F, Griscelli F, Ng LG, Zhang Z, Bost P, Amit I, Barlesi F, Marabelle A, Pène F, Gachot B, André F, Zitvogel L, Ginhoux F, Fontenay M, Solary E. 2020. Elevated Calprotectin and Abnormal Myeloid Cell Subsets Discriminate Severe from Mild COVID-19. Cell 182:1401–1418.e18.

23. King AMQ, Lefkowitz EJ, Mushegian AR, Adams MJ, Dutilh BE, Gorbalenya AE, Harrach B, Harrison RL, Junglen S, Knowles NJ, Kropinski AM, Krupovic M, Kuhn JH, Nibert ML, Rubino L, Sabanadzovic S, Sanfaçon H, Siddell SG, Simmonds P, Varsani A, Zerbini FM, Davison AJ. 2018. Changes to taxonomy and the International Code of Virus Classification and Nomenclature ratified by the International Committee on Taxonomy of Viruses (2018). Arch Virol 163:2601–2631.

24. Wang N, Shang J, Jiang S, Du L. 2020. Subunit Vaccines Against Emerging Pathogenic Human Coronaviruses. Front Microbiol 11:515400.

25. Lau SKP, Woo PCY, Li KSM, Huang Y, Tsoi H-W, Wong BHL, Wong SSY, Leung S-Y, Chan K-H, Yuen K-Y. 2005. Severe acute respiratory syndrome coronavirus-like virus in Chinese horseshoe bats. Proc Natl Acad Sci U S A 102:14040–14045.

26. Sharma A, Ahmad Farouk I, Lal SK. 2021. COVID-19: A Review on the Novel Coronavirus Disease Evolution, Transmission, Detection, Control and Prevention. Viruses 13.

27. Holmes EC, Goldstein SA, Rasmussen AL, Robertson DL, Crits-Christoph A, Wertheim JO, Anthony SJ, Barclay WS, Boni MF, Doherty PC, Farrar J, Geoghegan JL, Jiang X, Leibowitz

JL, Neil SJD, Skern T, Weiss SR, Worobey M, Andersen KG, Garry RF, Rambaut A. 2021. The origins of SARS-CoV-2: A critical review. Cell 184:4848–4856.

28. Menachery VD, Yount BL Jr, Sims AC, Debbink K, Agnihothram SS, Gralinski LE, Graham RL, Scobey T, Plante JA, Royal SR, Swanstrom J, Sheahan TP, Pickles RJ, Corti D, Randell SH, Lanzavecchia A, Marasco WA, Baric RS. 2016. SARS-like WIV1-CoV poised for human emergence. Proc Natl Acad Sci U S A 113:3048–3053.

29. Menachery VD, Yount BL Jr, Debbink K, Agnihothram S, Gralinski LE, Plante JA, Graham RL, Scobey T, Ge X-Y, Donaldson EF, Randell SH, Lanzavecchia A, Marasco WA, Shi Z-L, Baric RS. 2015. A SARS-like cluster of circulating bat coronaviruses shows potential for human emergence. Nat Med 21:1508–1513.

30. He B, Zhang Y, Xu L, Yang W, Yang F, Feng Y, Xia L, Zhou J, Zhen W, Feng Y, Guo H, Zhang H, Tu C. 2014. Identification of diverse alphacoronaviruses and genomic characterization of a novel severe acute respiratory syndrome-like coronavirus from bats in China. J Virol 88:7070–7082.

31. V'kovski P, Kratzel A, Steiner S, Stalder H, Thiel V. 2021. Coronavirus biology and replication: implications for SARS-CoV-2. Nat Rev Microbiol 19:155–170.

32. Malone B, Urakova N, Snijder EJ, Campbell EA. 2022. Structures and functions of coronavirus replication-transcription complexes and their relevance for SARS-CoV-2 drug design. Nat Rev Mol Cell Biol 23:21–39.

33. Totura AL, Baric RS. 2012. SARS coronavirus pathogenesis: host innate immune responses and viral antagonism of interferon. Curr Opin Virol 2:264–275.

34. Fehr AR, Perlman S. 2015. Coronaviruses: an overview of their replication and pathogenesis. Methods Mol Biol 1282:1–23.

35. Siu YL, Teoh KT, Lo J, Chan CM, Kien F, Escriou N, Tsao SW, Nicholls JM, Altmeyer R, Peiris JSM, Bruzzone R, Nal B. 2008. The M, E, and N structural proteins of the severe acute respiratory syndrome coronavirus are required for efficient assembly, trafficking, and release of virus-like particles. J Virol 82:11318–11330.

36. Schäfer A, Baric RS. 2017. Epigenetic Landscape during Coronavirus Infection. Pathogens 6:8.

37. Ramakrishnan V. 1997. Histone structure and the organization of the nucleosome. Annu Rev Biophys Biomol Struct 26:83–112.

38. Bell O, Tiwari VK, Thomä NH, Schübeler D. 2011. Determinants and dynamics of genome accessibility. Nat Rev Genet 12:554–564.

39. Kornberg RD, Lorch Y. 1999. Twenty-five years of the nucleosome, fundamental particle of the eukaryote chromosome. Cell 98:285–294.

40. Kaplan N, Moore IK, Fondufe-Mittendorf Y, Gossett AJ, Tillo D, Field Y, LeProust EM, Hughes TR, Lieb JD, Widom J, Segal E. 2009. The DNA-encoded nucleosome organization of a eukaryotic genome. Nature 458:362–366.

41. Lorch Y, LaPointe JW, Kornberg RD. 1987. Nucleosomes inhibit the initiation of transcription but allow chain elongation with the displacement of histones. Cell 49:203–210.

42. Han M, Grunstein M. 1988. Nucleosome loss activates yeast downstream promoters in vivo. Cell 55:1137–1145.

43. Schones DE, Cui K, Cuddapah S, Roh T-Y, Barski A, Wang Z, Wei G, Zhao K. 2008. Dynamic regulation of nucleosome positioning in the human genome. Cell 132:887–898.

44. Jiang C, Pugh BF. 2009. Nucleosome positioning and gene regulation: advances through

genomics. Nature reviews Genetics 10.

45. Krebs AR, Imanci D, Hoerner L, Gaidatzis D, Burger L, Schübeler D. 2017. Genome-wide Single-Molecule Footprinting Reveals High RNA Polymerase II Turnover at Paused Promoters. Mol Cell 67:411–422.e4.

46. Jaenisch R, Bird A. 2003. Epigenetic regulation of gene expression: how the genome integrates intrinsic and environmental signals. Nat Genet 33 Suppl:245–254.

47. Jones PA. 2012. Functions of DNA methylation: islands, start sites, gene bodies and beyond. Nat Rev Genet 13:484–492.

48. Deaton AM, Bird A. 2011. CpG islands and the regulation of transcription. Genes Dev 25:1010–1022.

49. Bernstein BE, Meissner A, Lander ES. 2007. The mammalian epigenome. Cell 128:669–681.

50. Barski A, Cuddapah S, Cui K, Roh T-Y, Schones DE, Wang Z, Wei G, Chepelev I, Zhao K. 2007. High-resolution profiling of histone methylations in the human genome. Cell 129:823–837.

51. Jenuwein T, Allis CD. 2001. Translating the histone code. Science 293:1074–1080.

52. Geisler S, Coller J. 2013. RNA in unexpected places: long non-coding RNA functions in diverse cellular contexts. Nat Rev Mol Cell Biol 14:699–712.

53. Sato F, Tsuchiya S, Meltzer SJ, Shimizu K. 2011. MicroRNAs and epigenetics. FEBS J 278:1598–1609.

54. Liu N, Pan T. 2015. RNA epigenetics. Translational research : the journal of laboratory and

clinical medicine 165.

55. Menachery VD, Eisfeld AJ, Schäfer A, Josset L, Sims AC, Proll S, Fan S, Li C, Neumann G, Tilton SC, Chang J, Gralinski LE, Long C, Green R, Williams CM, Weiss J, Matzke MM, Webb-Robertson B-J, Schepmoes AA, Shukla AK, Metz TO, Smith RD, Waters KM, Katze MG, Kawaoka Y, Baric RS. 2014. Pathogenic influenza viruses and coronaviruses utilize similar and contrasting approaches to control interferon-stimulated gene responses. mBio 5:e01174–14.

56. Poppe M, Wittig S, Jurida L, Bartkuhn M, Wilhelm J, Müller H, Beuerlein K, Karl N, Bhuju S, Ziebuhr J, Lienhard Schmitz M, Kracht M. 2017. The NF-κB-dependent and -independent transcriptome and chromatin landscapes of human coronavirus 229E-infected cells. PLoS Pathogens 13:e1006286.

57. Hou J, Wei Y, Zou J, Jaffery R, Sun L, Liang S, Zheng N, Guerrero AM, Egan NA, Bohat R, Chen S, Zheng C, Mao X, Yi SS, Chen K, McGrail DJ, Sahni N, Shi PY, Chen Y, Xie X, Peng W. 2024. Integrated multi-omics analyses identify anti-viral host factors and pathways controlling SARS-CoV-2 infection. Nature communications 15.

58. Chan K, Farias AG, Lee H, Guvenc F, Mero P, Brown KR, Ward H, Billmann M, Aulakh K, Astori A, Haider S, Marcon E, Braunschweig U, Pu S, Habsid A, Ah YT, Christie-Holmes N, Budylowski P, Ghalami A, Mubareka S, Maguire F, Banerjee A, Mossman KL, Greenblatt J, Gray-Owen SD, Raught B, Blencowe BJ, Taipale M, Myers C, Moffat J. 2023. Survival-based CRISPR genetic screens across a panel of permissive cell lines identify common and cell-specific SARS-CoV-2 host factors. Heliyon 9.

59. Wei J, Alfajaro MM, DeWeirdt PC, Hanna RE, Lu-Culligan WJ, Cai WL, Strine MS, Zhang S-M, Graziano VR, Schmitz CO, Chen JS, Mankowski MC, Filler RB, Ravindra NG, Gasque

V, de Miguel FJ, Patil A, Chen H, Oguntuyo KY, Abriola L, Surovtseva YV, Orchard RC, Lee B, Lindenbach BD, Politi K, van Dijk D, Kadoch C, Simon MD, Yan Q, Doench JG, Wilen CB. 2021. Genome-wide CRISPR Screens Reveal Host Factors Critical for SARS-CoV-2 Infection. Cell 184:76–91.e13.

60. You M, Chen L, Zhang D, Zhao P, Chen Z, Qin E-Q, Gao Y, Davis MM, Yang P. 2021. Single-cell epigenomic landscape of peripheral immune cells reveals establishment of trained immunity in individuals convalescing from COVID-19. Nat Cell Biol 23:620–630.

61. Li S, Wu B, Ling Y, Guo M, Qin B, Ren X, Wang C, Yang H, Chen L, Liao Y, Liu Y, Peng X, Xu C, Wang Z, Shen Y, Chen J, Liu L, Niu B, Zhu M, Liu L, Li F, Zhu T, Zhu Z, Zhou X, Lu H. 2021. Epigenetic Landscapes of Single-Cell Chromatin Accessibility and Transcriptomic Immune Profiles of T Cells in COVID-19 Patients. Front Immunol 12:625881.

62. Giroux NS, Ding S, McClain MT, Burke TW, Petzold E, Chung HA, Rivera GO, Wang E, Xi R, Bose S, Rotstein T, Nicholson BP, Chen T, Henao R, Sempowski GD, Denny TN, De Ussel MI, Satterwhite LL, Ko ER, Ginsburg GS, Kraft BD, Tsalik EL, Shen X, Woods CW. 2022. Differential chromatin accessibility in peripheral blood mononuclear cells underlies COVID-19 disease severity prior to seroconversion. Sci Rep 12:11714.

63. Chiariello AM, Abraham A, Bianco S, Esposito A, Fontana A, Vercellone F, Conte M, Nicodemi M. 2024. Multiscale modelling of chromatin 4D organization in SARS-CoV-2 infected cells. Nature communications 15.

64. Wang R, Lee JH, Kim J, Xiong F, Hasani LA, Shi Y, Simpson EN, Zhu X, Chen YT, Shivshankar P, Krakowiak J, Wang Y, Gilbert DM, Yuan X, Eltzschig HK, Li W. 2023. SARS-CoV-2 restructures host chromatin architecture. Nature microbiology 8.

65. Singhal A, Roth C, Micheva-Viteva SN, Venu V, Lappala A, Lee JT, Starkenburg SR,

Steadman CR, Sanbonmatsu KY. 2024. Human Coronavirus Infection Reorganizes Spatial Genomic Architecture in Permissive Lung Cells. Research Square rs.3.rs–3979539.

66. Zazhytska M, Kodra A, Hoagland DA, Frere J, Fullard JF, Shayya H, McArthur NG, Moeller R, Uhl S, Omer AD, Gottesman ME, Firestein S, Gong Q, Canoll PD, Goldman JE, Roussos P, tenOever BR, Jonathan B Overdevest, Lomvardas S. 2022. Non-cell-autonomous disruption of nuclear architecture as a potential cause of COVID-19-induced anosmia. Cell 185:1052–1064.e12.

67. Kee J, Thudium S, Renner DM, Glastad K, Palozola K, Zhang Z, Li Y, Lan Y, Cesare J, Poleshko A, Kiseleva AA, Truitt R, Cardenas-Diaz FL, Zhang X, Xie X, Kotton DN, Alysandratos KD, Epstein JA, Shi P-Y, Yang W, Morrisey E, Garcia BA, Berger SL, Weiss SR, Korb E. 2022. SARS-CoV-2 disrupts host epigenetic regulation via histone mimicry. Nature 610:381–388.

68. Finkel Y, Gluck A, Nachshon A, Winkler R, Fisher T, Rozman B, Mizrahi O, Lubelsky Y, Zuckerman B, Slobodin B, Yahalom-Ronen Y, Tamir H, Ulitsky I, Israely T, Paran N, Schwartz M, Stern-Ginossar N. 2021. SARS-CoV-2 uses a multipronged strategy to impede host protein synthesis. Nature 594:240–245.

69. Lapointe CP, Grosely R, Johnson AG, Wang J, Fernández IS, Puglisi JD. 2021. Dynamic competition between SARS-CoV-2 NSP1 and mRNA on the human ribosome inhibits translation initiation. Proc Natl Acad Sci U S A 118.

70. Abaeva IS, Arhab Y, Miścicka A, Hellen CUT, Pestova TV. 2023. reconstitution of SARS CoV-2 Nsp1-induced mRNA cleavage reveals the key roles of the N-terminal domain of Nsp1 and the RRM domain of eIF3g. bioRxiv.

71. Fisher T, Gluck A, Narayanan K, Kuroda M, Nachshon A, Hsu JC, Halfmann PJ,

Yahalom-Ronen Y, Tamir H, Finkel Y, Schwartz M, Weiss S, Tseng C-TK, Israely T, Paran N, Kawaoka Y, Makino S, Stern-Ginossar N. 2022. Parsing the role of NSP1 in SARS-CoV-2 infection. Cell Rep 39:110954.

72. Zhang K, Miorin L, Makio T, Dehghan I, Gao S, Xie Y, Zhong H, Esparza M, Kehrer T, Kumar A, Hobman TC, Ptak C, Gao B, Minna JD, Chen Z, García-Sastre A, Ren Y, Wozniak RW, Fontoura BMA. 2021. Nsp1 protein of SARS-CoV-2 disrupts the mRNA export machinery to inhibit host gene expression. Sci Adv 7.

73. Xia H, Cao Z, Xie X, Zhang X, Chen JY-C, Wang H, Menachery VD, Rajsbaum R, Shi P-Y. 2020. Evasion of Type I Interferon by SARS-CoV-2. Cell Rep 33:108234.

74. Anastasakis DG, Benhalevy D, Çuburu N, Altan-Bonnet N, Hafner M. 2024. Epigenetic repression of antiviral genes by SARS-CoV-2 NSP1. PLoS One 19:e0297262.

75. Ivanov KI, Yang H, Sun R, Li C, Guo D. 2024. The emerging role of SARS-CoV-2 nonstructural protein 1 (nsp1) in epigenetic regulation of host gene expression. FEMS Microbiology Reviews 48:fuae023.

76. Hoffmann H-H, Sánchez-Rivera FJ, Schneider WM, Luna JM, Soto-Feliciano YM, Ashbrook AW, Le Pen J, Leal AA, Ricardo-Lax I, Michailidis E, Hao Y, Stenzel AF, Peace A, Zuber J, David Allis C, Lowe SW, MacDonald MR, Poirier JT, Rice CM. 2020. Functional interrogation of a SARS-CoV-2 host protein interactome identifies unique and shared coronavirus host factors. Cell Host & Microbe 29:267.

77. McBride R, van Zyl M, Fielding BC. 2014. The coronavirus nucleocapsid is a multifunctional protein. Viruses 6:2991–3018.

78. Schelle B, Karl N, Ludewig B, Siddell SG, Thiel V. 2005. Selective replication of coronavirus genomes that express nucleocapsid protein. J Virol 79:6620–6630.

79. Wu C-H, Chen P-J, Yeh S-H. 2014. Nucleocapsid phosphorylation and RNA helicase DDX1 recruitment enables coronavirus transition from discontinuous to continuous transcription. Cell Host Microbe 16:462–472.

80. Grossoehme NE, Li L, Keane SC, Liu P, Dann CE 3rd, Leibowitz JL, Giedroc DP. 2009. Coronavirus N protein N-terminal domain (NTD) specifically binds the transcriptional regulatory sequence (TRS) and melts TRS-cTRS RNA duplexes. J Mol Biol 394:544–557.

81. Zúñiga S, Cruz JLG, Sola I, Mateos-Gómez PA, Palacio L, Enjuanes L. 2010. Coronavirus nucleocapsid protein facilitates template switching and is required for efficient transcription. J Virol 84:2169–2175.

82. Narayanan K, Maeda A, Maeda J, Makino S. 2000. Characterization of the coronavirus M protein and nucleocapsid interaction in infected cells. J Virol 74:8127–8134.

83. Baric RS, Nelson GW, Fleming JO, Deans RJ, Keck JG, Casteel N, Stohlman SA. 1988. Interactions between coronavirus nucleocapsid protein and viral RNAs: implications for viral transcription. J Virol 62:4280–4287.

84. Cologna R, Spagnolo JF, Hogue BG. 2000. Identification of nucleocapsid binding sites within coronavirus-defective genomes. Virology 277:235–249.

85. Karwaciak I, Sałkowska A, Karaś K, Dastych J, Ratajewski M. 2021. Nucleocapsid and Spike Proteins of the Coronavirus SARS-CoV-2 Induce in Monocytes and Macrophages-Potential Implications for Cytokine Storm Syndrome. Vaccines (Basel) 9.

86. Nilsson-Payant BE, Uhl S, Grimont A, Doane AS, Cohen P, Patel RS, Higgins CA, Acklin JA, Bram Y, Chandar V, Blanco-Melo D, Panis M, Lim JK, Elemento O, Schwartz RE, Rosenberg BR, Chandwani R, tenOever BR. 2021. The NF-κB Transcriptional Footprint Is Essential for SARS-CoV-2 Replication. J Virol 95:e0125721.

87. Hu Y, Li W, Gao T, Cui Y, Jin Y, Li P, Ma Q, Liu X, Cao C. 2017. The Severe Acute Respiratory Syndrome Coronavirus Nucleocapsid Inhibits Type I Interferon Production by Interfering with TRIM25-Mediated RIG-I Ubiquitination. J Virol 91.

88. Liu Y, Liang Q-Z, Lu W, Yang Y-L, Chen R, Huang Y-W, Wang B. 2021. A Comparative Analysis of Coronavirus Nucleocapsid (N) Proteins Reveals the SADS-CoV N Protein Antagonizes IFN-β Production by Inducing Ubiquitination of RIG-I. Frontiers in Immunology 12:688758.

89. Kopecky-Bromberg SA, Martínez-Sobrido L, Frieman M, Baric RA, Palese P. 2007. Severe acute respiratory syndrome coronavirus open reading frame (ORF) 3b, ORF 6, and nucleocapsid proteins function as interferon antagonists. J Virol 81:548–557.

90. Shivaswamy S, Bhinge A, Zhao Y, Jones S, Hirst M, Iyer VR. 2008. Dynamic Remodeling of Individual Nucleosomes Across a Eukaryotic Genome in Response to Transcriptional Perturbation. PLoS Biology 6:e65.

91. Vera DL, Madzima TF, Labonne JD, Alam MP, Hoffman GG, Girimurugan SB, Zhang J, McGinnis KM, Dennis JH, Bass HW. 2014. Differential nuclease sensitivity profiling of chromatin reveals biochemical footprints coupled to gene expression and functional DNA elements in maize. Plant Cell 26:3883–3893.

92. Turpin ZM, Vera DL, Savadel SD, Lung P-Y, Wear EE, Mickelson-Young L, Thompson WF, Hanley-Bowdoin L, Dennis JH, Zhang J, Bass HW. 2018. Chromatin structure profile data from DNS-seq: Differential nuclease sensitivity mapping of four reference tissues of B73 maize (L). Data Brief 20:358–363.

93. Cole L, Dennis J. 2020. MNase Profiling of Promoter Chromatin in -Stimulated GM12878 Cells Reveals Dynamic and Response-Specific Nucleosome Architecture. G3 (Bethesda)

10:2171–2178.

94. Cole L, Kurscheid S, Nekrasov M, Domaschenz R, Vera DL, Dennis JH, Tremethick DJ. 2021. Multiple roles of H2A.Z in regulating promoter chromatin architecture in human cells. Nat Commun 12:2524.

95. Mieczkowski J, Cook A, Bowman SK, Mueller B, Alver BH, Kundu S, Deaton AM, Urban JA, Larschan E, Park PJ, Kingston RE, Tolstorukov MY. 2016. MNase titration reveals differences between nucleosome occupancy and chromatin accessibility. Nat Commun 7:11485.

96. Brahma S, Henikoff S. 2019. RSC-Associated Subnucleosomes Define MNase-Sensitive Promoters in Yeast. Mol Cell 73:238–249.e3.

97. Sexton BS, Druliner BR, Vera DL, Avey D, Zhu F, Dennis JH. 2016. Hierarchical regulation of the genome: global changes in nucleosome organization potentiate genome response. Oncotarget 7:6460.

98. Druliner BR, Vera D, Johnson R, Ruan X, Apone LM, Dimalanta ET, Stewart FJ, Boardman L, Dennis JH. 2016. Comprehensive nucleosome mapping of the human genome in cancer progression. Oncotarget 7:13429.

99. Bolger AM, Lohse M, Usadel B. 2014. Trimmomatic: a flexible trimmer for Illumina sequence data. Bioinformatics 30:2114–2120.

100. Langmead B, Salzberg SL. 2012. Fast gapped-read alignment with Bowtie 2. Nat Methods 9:357–359.

101. Li H, Handsaker B, Wysoker A, Fennell T, Ruan J, Homer N, Marth G, Abecasis G, Durbin R, 1000 Genome Project Data Processing Subgroup. 2009. The Sequence

Alignment/Map format and SAMtools. Bioinformatics 25:2078–2079.

102. Chen K, Xi Y, Pan X, Li Z, Kaestner K, Tyler J, Dent S, He X, Li W. 2013. DANPOS: dynamic analysis of nucleosome position and occupancy by sequencing. Genome Res 23:341–351.

103. Ramírez F, Dündar F, Diehl S, Grüning BA, Manke T. 2014. deepTools: a flexible platform for exploring deep-sequencing data. Nucleic Acids Res 42:W187–91.

104. Kramer NE, Davis ES, Wenger CD, Deoudes EM, Parker SM, Love MI, Phanstiel DH. 2022. Plotgardener: cultivating precise multi-panel figures in R. Bioinformatics 38:2042–2045.

105. Raney BJ, Barber GP, Benet-Pagès A, Casper J, Clawson H, Cline MS, Diekhans M, Fischer C, Navarro GJ, Hickey G, Hinrichs AS, Kuhn RM, Lee BT, Lee CM, Le Mercier P, Miga KH, Nassar LR, Nejad P, Paten B, Perez G, Schmelter D, Speir ML, Wick BD, Zweig AS, Haussler D, Kent WJ, Haeussler M. 2024. The UCSC Genome Browser database: 2024 update. Nucleic Acids Res 52.

106. Chen EY, Tan CM, Kou Y, Duan Q, Wang Z, Meirelles GV, Clark NR, Ma'ayan A. 2013. Enrichr: interactive and collaborative HTML5 gene list enrichment analysis tool. BMC Bioinformatics 14:128.

107. Sloan CA, Chan ET, Davidson JM, Malladi VS, Strattan JS, Hitz BC, Gabdank I, Narayanan AK, Ho M, Lee BT, Rowe LD, Dreszer TR, Roe G, Podduturi NR, Tanaka F, Hong EL, Cherry JM. 2016. ENCODE data at the ENCODE portal. Nucleic Acids Res 44:D726–32.

108. Luo Y, Hitz BC, Gabdank I, Hilton JA, Kagda MS, Lam B, Myers Z, Sud P, Jou J, Lin K, Baymuradov UK, Graham K, Litton C, Miyasato SR, Strattan JS, Jolanki O, Lee J-W,

Tanaka FY, Adenekan P, O'Neill E, Cherry JM. 2020. New developments on the Encyclopedia of DNA Elements (ENCODE) data portal. Nucleic Acids Res 48:D882–D889.

109. Gordon DE, Jang GM, Bouhaddou M, Xu J, Obernier K, White KM, O'Meara MJ, Rezelj VV, Guo JZ, Swaney DL, Tummino TA, Hüttenhain R, Kaake RM, Richards AL, Tutuncuoglu B, Foussard H, Batra J, Haas K, Modak M, Kim M, Haas P, Polacco BJ, Braberg H, Fabius JM, Eckhardt M, Soucheray M, Bennett MJ, Cakir M, McGregor MJ, Li Q, Meyer B, Roesch F, Vallet T, Mac Kain A, Miorin L, Moreno E, Naing ZZC, Zhou Y, Peng S, Shi Y, Zhang Z, Shen W, Kirby IT, Melnyk JE, Chorba JS, Lou K, Dai SA, Barrio-Hernandez I, Memon D, Hernandez-Armenta C, Lyu J, Mathy CJP, Perica T, Pilla KB, Ganesan SJ, Saltzberg DJ, Rakesh R, Liu X, Rosenthal SB, Calviello L, Venkataramanan S, Liboy-Lugo J, Lin Y, Huang X-P, Liu Y, Wankowicz SA, Bohn M, Safari M, Ugur FS, Koh C, Savar NS, Tran QD, Shengjuler D, Fletcher SJ, O'Neal MC, Cai Y, Chang JCJ, Broadhurst DJ, Klippsten S, Sharp PP, Wenzell NA, Kuzuoglu-Ozturk D, Wang H-Y, Trenker R, Young JM, Cavero DA, Hiatt J, Roth TL, Rathore U, Subramanian A, Noack J, Hubert M, Stroud RM, Frankel AD, Rosenberg OS, Verba KA, Agard DA, Ott M, Emerman M, Jura N, von Zastrow M, Verdin E, Ashworth A, Schwartz O, d'Enfert C, Mukherjee S, Jacobson M, Malik HS, Fujimori DG, Ideker T, Craik CS, Floor SN, Fraser JS, Gross JD, Sali A, Roth BL, Ruggero D, Taunton J, Kortemme T, Beltrao P, Vignuzzi M, García-Sastre A, Shokat KM, Shoichet BK, Krogan NJ. 2020. A SARS-CoV-2 protein interaction map reveals targets for drug repurposing. Nature 583:459–468.

110. Yedidya Y, Davis D, Drier Y. 2023. SARS-CoV-2 infection perturbs enhancer mediated transcriptional regulation of key pathways. PLoS computational biology 19.

111. Pi P, Zeng Z, Zeng L, Han B, Bai X, Xu S. 2023. Molecular mechanisms of COVID-19-induced pulmonary fibrosis and epithelial-mesenchymal transition. Frontiers in

pharmacology 14.

112. D'Onofrio V, Sékaly RP. 2024. The immune-endocrine interplay in sex differential responses to viral infection and COVID-19. Trends in immunology 45.

113. Dhakal S, Ruiz-Bedoya CA, Zhou R, Creisher PS, Villano JS, Littlefield K, Ruelas CJ, Marinho P, Jedlicka AE, Ordonez AA, Bahr M, Majewska N, Betenbaugh MJ, Flavahan K, Mueller ARL, Looney MM, Quijada D, Mota F, Beck SE, Brockhurst J, Braxton AM, Castell N, Stover M, D'Alessio FR, Ka MP, Karakousis PC, Mankowski JL, Pekosz A, Jain SK, Klein SL. 2021. Sex Differences in Lung Imaging and SARS-CoV-2 Antibody Responses in a COVID-19 Golden Syrian Hamster Model. mBio 12.

114. Wang X, Liu Y, Li K, Hao Z. 2023. Roles of p53-Mediated Host-Virus Interaction in Coronavirus Infection. International journal of molecular sciences 24.

115. Lodhi N, Singh R, Rajput SP, Saquib Q. 2021. SARS-CoV-2: Understanding the Transcriptional Regulation of ACE2 and TMPRSS2 and the Role of Single Nucleotide Polymorphism (SNP) at Codon 72 of p53 in the Innate Immune Response against Virus Infection. Int J Mol Sci 22.

116. Alnajeebi AM, Alharbi HFH, Alelwani W, Babteen NA, Alansari WS, Shamlan G, Eskandrani AA. 2022. COVID-19 Candidate Genes and Pathways Potentially Share the Association with Lung Cancer. Comb Chem High Throughput Screen 25:2463–2472.

117. Schultheiß C, Willscher E, Paschold L, Gottschick C, Klee B, Glasauer S, Henkes S-S, Bosurgi L, Dutzmann J, Sedding DG, Frese T, Girndt M, Höll JI, Gekle M, Mikolajczyk R, Binder M. 2021. From online data collection to identification of disease mechanisms: The IL-1ß, IL-6 and TNF-α cytokine triad is associated with post-acute sequelae of COVID-19 in a digital research cohort. SSRN Electron J https://doi.org/10.2139/ssrn.3963839.

118. Hu B, Guo H, Zhou P, Shi ZL. 2021. Characteristics of SARS-CoV-2 and COVID-19. Nature reviews Microbiology 19.

119. Kumar A, Grams TR, Bloom DC, Toth Z. 2022. Signaling Pathway Reporter Screen with SARS-CoV-2 Proteins Identifies nsp5 as a Repressor of p53 Activity. Viruses 14:1039.

120. Luo H, Chen Q, Chen J, Chen K, Shen X, Jiang H. 2005. The nucleocapsid protein of SARS coronavirus has a high binding affinity to the human cellular heterogeneous nuclear ribonucleoprotein A1. FEBS letters 579.

121. 2020. SARS-CoV-2 Disrupts Splicing, Translation, and Protein Trafficking to Suppress Host Defenses. Cell 183:1325–1339.e21.

122. Zheng X, Sun Z, Yu L, Shi D, Zhu M, Yao H, Li L. 2021. Interactome Analysis of the Nucleocapsid Protein of SARS-CoV-2 Virus. Pathogens (Basel, Switzerland) 10.

123. Blagova O, Lutokhina Y, Kogan E, Savina P, Aleksandrova S, Zaklyazminskaya E. 2024. Post-COVID Myocarditis in Patients with Primary Cardiomyopathies: Diagnosis, Clinical Course and Outcomes. Genes 15.

124. Mezache L, Nuovo GJ, Suster D, Tili E, Awad H, Radwański PB, Veeraraghavan R. 2022. Histologic, viral, and molecular correlates of heart disease in fatal COVID-19. Annals of diagnostic pathology 60.

125. Yan HW, Feng YD, Tang N, Cao FC, Lei YF, Cao W, Li XQ. 2024. Viral myocarditis: From molecular mechanisms to therapeutic prospects. European journal of pharmacology 982.

126. Butowt R, Bilinska K, von Bartheld CS. 2023. Olfactory dysfunction in COVID-19: new insights into the underlying mechanisms. Trends in neurosciences 46.

127. Ajaz S, McPhail MJ, Singh KK, Mujib S, Trovato FM, Napoli S, Agarwal K. 2020. Mitochondrial metabolic manipulation by SARS-CoV-2 in peripheral blood mononuclear cells of patients with COVID-19. American Journal of Physiology - Cell Physiology 320:C57.

128. Gibellini L, De Biasi S, Paolini A, Borella R, Boraldi F, Mattioli M, Lo Tartaro D, Fidanza L, Caro-Maldonado A, Meschiari M, Iadisernia V, Bacca E, Riva G, Cicchetti L, Quaglino D, Guaraldi G, Busani S, Girardis M, Mussini C, Cossarizza A. 2020. Altered bioenergetics and mitochondrial dysfunction of monocytes in patients with COVID-19 pneumonia. EMBO molecular medicine 12.

129. Zhou S, Hui X, Wang W, Zhao C, Jin M, Qin Y, Chen M. 2025. SARS-CoV-2 and HCoV-OC43 regulate host m6A modification via activation of the mTORC1 signaling pathway to facilitate viral replication. Emerging microbes & infections https://doi.org/10.1080/22221751.2024.2447620.

130. Madeddu E, Maniga B, Zaffanello M, Fanos V, Marcialis A. 2022. The SARS-CoV2 and mitochondria: the impact on cell fate. Acta bio-medica : Atenei Parmensis 93.

131. Sarker B, Rahaman MM, Islam MA, Alamin MH, Husain MM, Ferdousi F, Ahsan MA, Mollah MNH. 2023. Identification of host genomic biomarkers from multiple transcriptomics datasets for diagnosis and therapies of SARS-CoV-2 infections. PloS one 18.